2014-01-01

Global Sphingolipid Profile of Giardia lamblia During Stage Differentiation: The influence of Sphingomyelin Abundance on Viable Cyst Production

Trevor Thomas Duarte
University of Texas at El Paso, ttduarte@miners.utep.edu

GLOBAL SPHINGOLIPID PROFILE OF *GIARDIA LAMBLIA* DURING STAGE DIFFERENTIATION: THE INFLUENCE OF SPHINGOMYELIN ABUNDANCE ON CYST VIABILITY

TREVOR THOMAS DUARTE

Department of Biological Science

APPROVED:

Siddhartha Das, Ph.D., Chair

Igor C. Almeida, Ph.D.

Rosa A. Maldonado, D.Sc.

Renato Aguilera, Ph.D.

Katja Michael, Ph.D.

Bess Sirmon-Taylor, Ph.D.
Interim Dean of the Graduate School

Dedication

To Minerva and Aurelio.

GLOBAL SPHINGOLIPID PROFILE OF *GIARDIA LAMBLIA* DURING STAGE DIFFERENTIATION: THE INFLUENCE OF SPHINGOMYELIN ABUNDANCE ON CYST VIABILITY

by

TREVOR THOMAS DUARTE, BS

DISSERTATION

Presented to the Faculty of the Graduate School of

The University of Texas at El Paso

in Partial Fulfillment

of the Requirements

for the Degree of

DOCTOR OF PHILOSPHY

Department of Biological Science

THE UNIVERSITY OF TEXAS AT EL PASO

May 2014

Acknowledgements

I would like to thank all of the people who made this work possible. First special thanks to my wife Minerva and my son Aurelio for reminding me not to bring home any "fukalanga" and listening to me go on and on about sphingolipids so that I wasn't talking to myself. Mil gracias a mis suegros Adrián y Martha Laveaga por su apoyo y gracias también a mis cuñados Adrián y Fabian Laveaga y mi cuñada Verónica Cano. Sincere thank you to my parents Debi and Michael Duarte and Thomas Crater and my brother Josh Crater.

I'd like to thank the members of the Das lab whose generosity with their time was unbelievable, especially Dr. Tavis Mendez and Mr. Christiancel Salazar as well as other current members Dr. Atasi De Chatterjee, Mr. Joaquin De Leon, Ms. Monica Delgado, Dr. Leobarda Robles-Martinez, Mr. Duran Debons and past members Dr. Yuni Hernandez, seriously the nicest person I've ever met, Drs. Debarshi Roy and Suparna Ray. Great thanks to Mr. Felipe Gazos Lopez for the many hours of stimulating conversation about science, politics and literature. Thank you to Dr. Armando Varela for never telling me to come back later and Dr. Emma Arrigi for sometimes doing just that. Thank you to Dr. Igor Almeida for trusting me to tinker with not one, but four mass spectrometers. To the faculty members who challenged me during my doctoral classes including Drs. Max Shpak, Tina Garza and German Rosas Acosta. Thank you to Dr. Elizabeth Walsh for your support of the students being like-minded about animal rights and being so easy to find. Thank you to my committee, Drs. Igor Almeida, Rosa Maldonado, Renato Aguilera and Katja Michael. I received funding from the RISE program as both an undergraduate and as a graduate student, thank you Dr. Renato Aguilera.

This dissertation would not have been possible without the unwavering financial, moral and intellectual support and guidance of Dr. Siddhartha Das. I could not have known when I started, how fortunate I was, thank you.

Abstract

Giardia lamblia is a protozoan parasite and a major cause of the waterborne-illness (known as giardiasis) worldwide. Giardiasis is endemic in developing countries and is a leading cause of non-viral- and non-bacterial-associated intestinal disorders. Acute symptoms of giardiasis include diarrhea, cramps, and malabsorption. The disease is often self-limiting, although the infection can result in long-term disorders such as chronic fatigue, stunted cognitive skills, and failure to thrive even after the parasite has been cleared.

This parasite exists in two morphologic forms—infective trophozoites and transmissible, water-resistant cyst, which is passed by the fecal-oral route and is likely to be spread by contaminated drinking water. Infection can occur upon ingestion of as few as 10 cysts, and an infected individual sheds more than 10^9 cysts in the feces per day. Although giardiasis can effectively be treated with nitroheterocyclic compounds, such drugs can cause unpleasant side effects and ultimately lead to drug-resistant parasites. Therefore, it is necessary to identify novel targets for developing new anti-giardial agents. One of these targets could be sphingolipid (SL) pathways because the results from our laboratory indicate that SL genes and gene products play critical roles in regulating encystation (cyst formation) of *Giardia.* We have shown previously that SL metabolism in *Giardia* is limited to five putative enzymes, which are differentially regulated during the formation of water-resistant cysts. We have also shown that the silencing of the giardial glucosylceramide synthase gene (gGlcT1) using anti-gGlcT1 morpholino oligonucleotide results in inhibition of growth and the production of viable cysts.

The goal of my dissertation is to establish the sphingolipidome of *Giardia* during encystation to provide a global perspective of the SL changes that take place during this critical stage of the parasite's life cycle and to show how *Giardia* can modulate these lipids. In Specific Aim 1, I used mass spectrometry to elucidate the sphingolipid profile of *Giardia* during encystation as well as culture media sources of SLs. In Specific Aim 2, I investigated the

parasite's ability to generate ceramide from the hydrolysis of sphingomyelin (SM) via two putative sphingomyelinase (SMase) enzymes identified by mining the *Giardia* genome project.

Briefly, I found that the levels of ceramide and glycosylceramides increased significantly (~10 fold) during encystation followed by a decline in cysts. The level of sphingomyelin (SM), on the other hand, increased sharply in the cyst population. Analysis indicated that SM-enriched cysts are viable and undergo excystation in culture. It was also observed that *Giardia* expresses two active acid SMase enzymes (gASMLPD3b1 and gASMLPD3b2) with distinct pH requirements, one of which shows the characteristics of a secreted SMase. My results indicate that a dynamic metabolic conversion among various classes of SLs occurs during giardial encystation, and that this conversion could be critical for completing excystation and producing infection in the human gut.

Table of Contents

List of Tables

List of Figures

List of Abbreviations

GalNAc, β(1-3)-N-acetyl-d-galactosamine
CWP1, cyst wall protein 1
CWP2, cyst wall protein 2
CWP3, cyst wall protein 3
ESV, encystation specific vesicle
h.p.i. hours post induction
PV, peripheral vacuole
TVN, tubular vesicle network
ER, endoplasmic reticulum
DNA, deoxyribonucleic acid
NO, nitric oxide
VSP, variable surface protein
SREBP, sterol regulatory element binding protein
HCNCp, high-cysteine non-variant cyst protein
ATP, Adenosine tri-phosphate
TLC, thin layer chromatography
qTOF, quadrupole time of flight
Lyso-PC, lyso-phosphatidylcholine
PC, phosphatidylcholine
PG, phosphatidylglycerol
PE, phosphatidylethanolamine
CDP-DAG, cytidine diphosphate-diacylglycerol
SM, sphingomyelin
Cer, Ceramide
PalmA, palmitic acid
SL, sphingolipid
gSPT1, giardial serine palmitoyltransferase 1
gSPT2, giardial serine palmitoyltransferase 2
gGlcT1, giardial glucosylceramide transferase 1
GCS, glucosylceramide synthase
gASMLPD3b1, giardial acid sphingomyelinase-like phosphodiesterase 3b 1
gASMLPD3b2, giardial acid sphingomyelinase-like phosphodiesterase 3b 2
SMPDL-3b, sphingomyelinase phosphodiesterase like 3b
SAGE, serial analysis of gene expression
qRT-PCR, quantitative reverse transcription polymerase chain reaction
PPMP, D-threo-1-phenyl-2-decanoylamino-3-morpholino-1-propano
GSLs, glycosphingolipids
3KSR, 3-ketosphinganine reductase
Lass, longevity assurance gene (dihydroceramide synthase)
CerS, ceramide synthase
CerK, ceramide kinase
SMase, sphingomyelinase

DAG, diacylglycerol
NBD, N-[7-(4-nitrobenzo-2-oxa-1,3-diazole)]
Bodipy, 4,4-difluoro-4-bora-3a,4a-diaza-s-indacene
PBS, phosphate buffered saline
PTFE, polytetrafluoroethylene
DEAE-CL, diethylaminoethyl-chloride
NaOAc, Sodium Acetate
DCE, dichloroethane
LTQ, linear triple quadrupole
TIM, total ion map
HPLC, high pressure liquid chromatography
SIM, select ion monitoring
LC MS/MS, tandem liquid chromatography mass spectrometry
SE, standard error
ESI, electrospray ionization
GM3, mono-sialo dihexosylceramide
GD3, di-sialo dihexosylceramide
GM1, mono-sialo HexNAc trihexosylceramide
LCB, long chain base
NL, neutral loss
BP, base peak
FSGS, focal segmental glomerulosclerosis
ASMase, acid sphingomyelinase
BSA, bovine serum albumin
IVT, *in vitro* translated
GFP, green fluorescent protein
HPTLC, high performance thin layer chromatography
PVDF, polyvinylidene fluoride
SDS-PAGE, sodium dodecyl sulfate-polyacrylamide gel electrophoresis
HRP, horse radish peroxidase
ECL, enhanced chemi-luminescence
PFA, paraformaldehyde
DAPI, 4', 6-diamidino-2-phenylindole
FDA, fluorescein diacetate
PI, propidium iodide
MS, mass spectrometry

Introduction

People, especially children, can die from diarrheal diseases. According to the World Health Organization (WHO), diarrhea is the second leading cause of death among children under five, killing an estimated 760,000 children every year (WHO Bulletin 2013). Diarrheal disease is caused by bacteria, viruses, and intestinal parasites, including *Giardia lamblia* (hereinafter *Giardia*), a causative agent of waterborne illness or "giardiasis." Giardiasis is classified under the "Neglected Tropical Diseases" category and is generally self-limiting, but recurrence is common in endemic areas (Watkins and Eckmann 2014). There is no vaccine, and treatment with common anti-parasitic agents is confounded by adverse side effects and decreasing drug susceptibility. Furthermore, intestinal micro flora plays an important role in determining the severity of giardial infection. For example recent evidence suggests that reduction of helminth infection may be associated with the increase of *Giardia* infection (Blackwell *et al.* 2013). Helminthes modulate host lipid levels in order to carry out their own cellular processes (reviewed by Bansal *et al.,* 2005). Similarly, *Giardia* uses the host's lipids for its growth and differentiation because it is unable to synthesize its own lipids *de novo* (Das *et al.* 2001; Yichoy *et al.* 2010). Thus, it is possible that the antagonism observed between these organisms involves competition for intestinal lipids, which they both colonize. Investigation into additional lipids essential for growth and/or differentiation of *Giardia* may provide insight into alternative strategies for combating this disease.

Giardia trophozoites colonize the intestine of mammalian hosts. This is a low-oxygen, nutrient-rich environment, in which the organism must contend not only with the host's immune response but also with the high levels of digestive enzymes constitutively secreted by the intestinal cells. The advantage, however, is that the parasite is able to scavenge these nutrients and thus accumulate metabolic energy that is required to synthesize organelles and macromolecules. A basal eukaryote *Giardia* lack both mitochondria and defined Golgi stack (Regoes *et al.* 2005; Reiner *et al.* 1990) although it is not clear if this is due to secondary loss as

a result of parasitism. What is clear is that the absence of these organelles, or their presence in rudimentary form, does not decrease fitness within the parasite. The same cannot be said for the host, where no benefit is gained from colonization by *Giardia*. In fact, acute giardiasis considerably reduces host fitness, and even after the infection has been cleared the evidence suggests that there are a number of long-term effects of infection, including irritable-bowel syndrome, chronic fatigue, and failure to thrive (Halliez and Buret 2013).

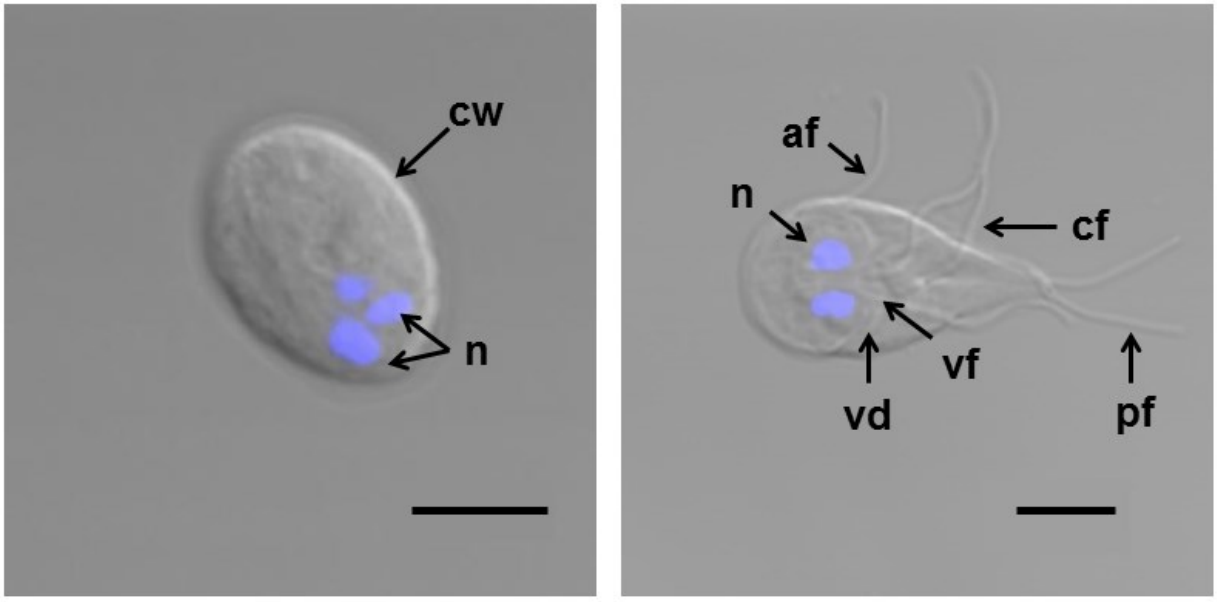

Figure 1.1: *Giardia* morphology

The giardial cyst (infectious stage) and trophozoite (vegetative stage). The active trophozoite stage contains two nuclei (n) and a ventral disc (vd) and ventral flagella (vf) for attachment. For movement the parasite relies on anterior (af), caudal (cf) and posterior flagella (pf). The dormant cyst contains four nuclei (n) enclosed within a cyst wall (cw).

Trophozoites in the intestine swim erratically by beating their flagella and attach to microvilli of intestinal epithelia using a suction-cup-like adhesive disc (House *et al.* 2011). While attached, the flagella continue to beat, and it has been suggested that this is the cause of the major symptoms of giardiasis: diarrhea and malabsorption (Ankarklev *et al.* 2010). It has

also been reported that *Giardia* secretes proteins *in vitro* when co-cultured with human epithelial cells, which can result in decreased membrane function and increased permeability (Ringqvist *et al.* 2008). However, no *Giardia* toxins capable of increasing membrane permeability have yet been identified.

For a pathogen to be successful, it must infect as many hosts as possible, and *Giardia* is no exception. However, sensitivity to oxygen and residence in the intestine pose an obstacle for the spread of this non-invasive parasite. To circumvent this, *Giardia* has a biphasic life cycle—the trophozoite is able to form a protective wall made of protein and polysaccharides by encystation. Although it is not known what triggers encystation, the induction of cyst formation *in vitro* described by Boucher and Gillin (1990) has allowed many groups to study this process using varied and sophisticated techniques. The formation of the cyst wall and the subsequent transformation to mature cyst takes place in the lower intestine (Adam 2001). The wall is composed of at least three secreted proteins (CWP1-3), as well as β(1-3)-N-acetyl-d-galactosamine (GalNAc) polymer (Gerwig *et al.* 2002; Gottig *et al.* 2006; Chatterjee *et al.* 2010). This appears to be a highly regulated process, in which the deposition of cyst-wall proteins (CWP1-3) and other materials occurs through concerted trafficking of these proteins in encystation-specific vesicles (ESV) during differentiation (Faso and Hehl 2011). Interestingly, polysaccharides are synthesized on the external surface of plasma membranes of trophozoites, but it is unclear when or how they are incorporated into the cyst wall. Usually, the deposition of the cyst wall is completed by 24-hour post-induction (h.p.i.) of *in vitro* encystation, and it coincides with dramatic morphologic changes as the flagellated trophozoite becomes an aflagellate, oval-shaped cyst, which is water resistant and capable of surviving in the oxidizing environment outside the host.

The cyst is passed by the fecal oral route, and therefore transmission is most often associated with infected water supplies as a result of poor or no treatment practices, poor separation of potable water and waste water lines, or communal bathing (Kramer *et al.* 1996; Karanis *et al.* 2007). As a source of infection and a cause of disease, *Giardia* is an important

organism to study in the hope that giardiasis can be prevented through medical intervention. A vaccine against *Giardia* is confounded by the expression of variable-surface proteins (VSPs), which allow *Giardia* to escape host adaptive immune responses (Prucca and Lujan 2009), but *Giardia* is a parasite and as such maintains only the metabolic pathways that are essential for growth. Thus, an integral part of combating the parasite is an understanding of the pathways that are maintained and those that have been forsaken. This provides a two-fold benefit to the study of this protozoan. First, *Giardia* is an evolutionarily conserved organism, the biology of which provides valuable insight into that of more derived organisms. Second, those pathways and processes maintained by *Giardia* are likely to yield targets for fighting the infection.

1.1 The Simple Life o*f Giardia lamblia*

The eukaryote parasite *Giardia intestinalis* (synonymous with *G. lamblia* and *G. duodenalis*) is a member of the diplomonada group, which also includes free-living organisms. The phylogenetic organization of *Giardia* is not clear, and it is not known whether the protist represents an evolutionarily basal organism that diverged before the mitochondrial fusion of higher eukaryotes or a more conserved organism with secondary loss of some organelles and metabolic pathways due to the parasitic life-style (Hilario and Gogarten 1998; Stechmann and Cavalier-Smith 2002). What is clear is that *Giardia* are minimal in a number of ways, including the lack of common eukaryote organelles, the maintenance and processing of genetic material, and the synthesis of proteins for both structure and metabolism.

Giardia does not possess mitochondria, and therefore it has traditionally been characterized as among the earliest branching eukaryotes. This has been called into question since the discovery of the mitochondria-like organelle, the mitosome (Regoes *et al.* 2005). Interestingly this organelle is not known to perform any of the functions traditionally associated with the mitochondria. No Golgi stack has been identified in *Giardia*. The closest to be found is a transient Golgi network, which appears during encystation and which has been implicated in the secretion of ESVs (Reiner *et al.* 1990; Stefanic *et al.* 2006). Rather than lysosomes, a series

of peripheral vacuoles (PVs) lie just below the plasma membrane. These PVs are continuous with the tubular vesicle network (TVN), which acts as both endoplasmic reticulum (ER) and endosome/lysosome (Abodeely *et al.* 2009).

The genome of this binucleate protist is compact, and it includes only four identified introns (Morrison *et al.* 2007). *Giardia* lacks the genes necessary for the synthesis of purines and pyrimidines, and therefore it must scavenge these from the environment. Although micro-aerophillic, they do not possess genes required for protection from oxidative stress, including catalase and superoxide dismutase (Brown *et al.* 1995). Furthermore, *Giardia* has a paucity of protein subunits for the formation of multi-meric complexes associated with a range of functions, including initiation of DNA replication, initiation of transcription, and poly-adenylation (Morrison *et al.* 2007).

1.2 Living Between Two Worlds

Infection with giardiasis can be the result of ingestion of less than 10 cysts (Talal and Murray 1994), which usually comes from drinking contaminated water. These cells have survived in an oxygen-rich environment in which temperatures are considerably lower than those found within the host. The cyst wall is constituted of 40% proteins and 60% polysaccharides, which makes the cysts osmotically-resistant. Upon ingestion, the cells pass through the low pH of the stomach, where it is believed that gastric acids begin to break down the wall. The process of exiting from the cyst, excystation, is completed after the cell has traveled through the stomach to the small intestine, where it is exposed to alkaline pH and digestive enzymes such as Trypsin. During this process, *Giardia* secretes lysosomal acid phosphatase to de-phosphorylate cyst wall proteins (Slavin *et al.* 2002), cathepsin B (Ward *et al.* 1997) to degrade these proteins, and a specific glycohydrylase to cleave GalNAc fibrils. Once finished, the exiting cell (excyzoites) has divided twice to produce four trophozoites.

It is in the intestine, just below the bile duct, where *Giardia* colonizes and causes disease. The trophozoite beats its flagella and uses its ventral disc like a suction cup to attach

itself (House *et al.* 2011). The host mounts an innate immune response, which is in part countered by the parasite's consumption of arginine, limiting host-cell production of Nitric Oxide (NO). It has also been suggested that secreted factors play a role in limiting host-cell immune response by altering membrane function (Ringqvist *et al.* 2008). Host adaptive immunity is confounded by clonal expression of continuously changing VSPs, which allow the parasite to evade recognition (Prucca and Lujan 2009). The final means by which *Giardia* escapes host defenses is to leave, and by doing so it spreads the infection. To do this, the cell undergoes considerable morphologic changes and forms the cyst wall. First, a transient Golgi network is developed to secrete ESVs—which carry CWP1-3—to the cell surface. It is interesting that these proteins are regulated by the sterol regulatory element binding protein (SREBP), which mediates post-translational modification of proteins through intermediates of cholesterol metabolism. Early morphological changes such as loss of ventral disc and flagellum cause the cell to detach from the intestinal epithelia (Lauwaet *et al.* 2007). This will probably cause the cell to pass from the small intestine through the middle intestine to the large intestine before reaching the colon. Ultimately, the cyst wall will be laid down, and it comprises the cyst-wall proteins, a high-cysteine non-variant cyst protein (HCNCp), giardial Myb2, cysteine-protease-2, novel cyst proteins with epidermal growth factor repeats, and Rab 11 (DuBois *et al.* 2008; Huang *et al.* 2008; Castillo-Romero *et al.* 2010). The remainder of the cyst wall is composed of lipids and carbohydrates. Sixty percent of the cyst wall consists of GalNAc fibrils (Gerwig *et al.* 2002) that are synthesized from fructose-6-phosphate by an unusual bacteria-like pathway (Lopez *et al.* 2007; Morrison *et al.* 2007). Unpublished data from our laboratory suggest that lipid comprises at least some of the cyst wall, based on the observation that FasDil, which is a lipid staining dye, binds to the cyst wall of in-vitro-derived cysts. However, isolation of lipids from the cyst wall for identification represents a significant challenge because in order to isolate cyst wall strong detergents are traditionally employed. Once the cyst wall is complete, the micro-aerophillic cell can safely survive in the oxidative environment outside of the host. As

many as 10^9 cysts are shed by infected humans per day (Karanis *et al.* 2007) to contaminate water supplies and thus complete the life cycle.

1.3 Lipid Synthesis and Scavenging

As stated above, *Giardia* colonizes the small intestine of mammalian hosts just below the bile duct. In this complex and harsh environment, the trophozoite has access to nutrients derived from the host diet, epithelial cells, and micro flora. Intake of these nutrients provides energy to *Giardia* in two forms: (1) through the metabolism of glucose to pyruvate through the Embden-Meyerhof-Parnas and hexose monophosphate shunt pathways (Lindmark 1980; Adam 2001), and (2) the conversion of arginine to ornithine, producing ATP (Schofield *et al.* 1992). Because of limited amino acid synthesis, the latter form of energy production competes with the host cell for arginine, an important substrate for epithelial cell NO synthesis, which in turn limits host defenses by reducing NO (Eckmann *et al.* 2000).

Apart from the glucose and arginine required for energy metabolism, *Giardia* is exposed to bile salts as well as dietary lipids and free fatty acids. The effects of these nutrients have been reported to both promote and retard *Giardia* growth and encystation. Fatty acids have been shown to have anti-giardial properties (Rayan *et al.* 2005) and to be detrimental for growth (Reiner *et al.* 1986; Das *et al.* 1988), and lauric acid (C12:0), for example, accumulates in trophozoites and alters the plasma membrane integrity. Alternatively, bile acids have been reported to promote the formation of mixed micelles, which facilitate the transport of intestinal lipids into *Giardia*. Bile and fatty acids are also established inducers of *in-vitro* encystation, as originally proposed by Gillin and colleagues (Gillin *et al.* 1986; Gillin 1987).

Lipid synthesis is limited in *Giardia* (Yichoy *et al.* 2011). Early studies using radioactive precursors showed that acetate, glucose, glycerol, threonine, cholesterol, and glycerol-3-phosphate failed to incorporate into other lipids, which provided evidence that *Giardia* is unable to synthesize lipids *de novo*. It was therefore postulated that *Giardia* acquires phospholipids and fatty acids from the culture media *in vitro* and from the host dietary lipids *in vivo* (Jarroll et al.

1981). This was supported by thin-layer chromatography (TLC) analysis, which showed a similar lipid profile between the growth media and the giardial cells (Kaneda and Goutsu 1988; Mohareb *et al.* 1991). Using quadrupole time-of-flight (qTOF) mass spectrometry, our laboratory has identified only lyso-phosphatidylcholine (lyso-PC) and phosphatidylcholine (PC) in the serum and bile, which suggests that the phosphatidylglycerol (PG) and phosphatidylethanolamine (PE) found in giardial cells were being synthesized by the parasite (Yichoy *et al.* 2009). We have proposed that these phospholipids could be generated via the fatty acid and head-group remodeling pathways by passing the CDP-DAG (*de novo*) pathway (Das *et al.* 2001). The support for this hypothesis is twofold. First, radio labelled fatty acids are readily incorporated into membrane phospholipids (Blair and Weller 1987; Stevens *et al.* 1997; Gibson *et al.* 1999; Vargas-Villarreal *et al.* 2007), and second, radiolabeled choline, ethanolamine, inositol, serine, and glycerol are readily incorporated into respective phospholipids in trophozoites when these bases are added to the culture media (Das *et al.,* unpublished). It follows that lipid neogenesis in *Giardia* is likely to be more often the result of fatty acid remodeling/head-group exchange than the result of the Lands cycle.

Scavenging of lipids is likely to provide an abundant source of lipids, as well as substrate for conversion to the lipids required by the organism. Using fluorescent analogues, our lab has shown that *Giardia* readily ingests and incorporates lipids throughout the cell. Cellular localization studies indicate that cellular targeting is distinct between lipid classes, which suggest at least some role for active transport of these lipids in and out of the cell. For example, although PC incorporates into the plasma membrane and flagella, sphingomyelin (SM), which also possesses the choline headgroup labels that the nuclear envelope and plasma membrane similar to palmitic acid (PalmA). PG and ceramide (Cer) both label the perinuclear membrane, and PE localizes to the plasma membrane and the discrete cytoplasmic structures just below the membrane (Stevens *et al.* 1997; Gibson *et al.* 1999; Das *et al.* 2001).

The mechanism by which lipids are incorporated into the cell varies between active and passive transport. Intracellular trafficking of Cer and SM was shown by our lab to be blocked by

the actin depolymerizing drug cytochalasin-D, which suggests that these lipids are endocytosed through cytoskeletal-dependent processes (Hernandez *et al.* 2007; Castillo-Romero *et al.* 2010). We reported that ceramide is internalized by clatherin-coated vesicles, which target the perinuclear membrane, and that the microtubule depolymerizing drugs also block the release of PG from the ER, which suggests that not only intake but also the transport of this lipid is cytoskeleton dependent. In contrast, neither PC nor palmitic acid was affected by anti-cytoskeletal agents, which suggests that the intake of these is not dependent upon the cytoskeleton for trafficking (Castillo-Romero *et al.* 2010).

1.4 Of Sphingolipids and Encystation

When the *Giardia* genome project was finished, it was possible to gain access to a plethora of information about the giardial genome as described above. Our lab's interest in lipids led us to investigate genes related to lipid metabolism in *Giardia,* and soon we identified an as-yet-undescribed gap in the metabolism of the highly bioactive sphingolipids (SLs). SLs are (1) lipids with a sphingosine base and an amide-linked fatty acid chain that are both structural as components of detergent-resistant membrane (DRM) microdomains, and (2) functional as important signaling molecules (Hannun and Obeid 2008; Lingwood and Simons 2010). According to data mining in the genome, *Giardia* is quite limited in the *de novo* synthesis and metabolism of SLs. *Giardia* maintains two copies of the enzyme responsible for the first committed step of SL synthesis—serine palmitoyltransferase (gSPT1 and gSPT2) and glucosylceramide transferase (gGlcT1 or GCS). Evidence for the metabolism of SLs is slightly more scarce, with two copies of an acid sphingomyelinase-like phosphodiesterase 3b precursor (gASMLPD3b1 and gASMLPD3b2). From this, it may seem that SL metabolism simply is not required by the parasite, but recent reports by our laboratory and others suggest that these genes are important for both giardial growth and encystation. Expression profiles using serial analysis of gene expression (SAGE), microarray, and quantitative real-time polymerase chain reaction (qRT-PCR) all indicate a differential transcription of giardial SL metabolic genes during cyst

formation (Hernandez *et al.* 2008; Birkeland *et al.* 2010; Morf *et al.* 2010). In addition, treatment of trophozoites with L-cycloserine, an inhibitor of SPT, has been shown to interrupt ceramide uptake and targeting (Hernandez *et al.* 2008). D-threo-1-phenyl-2-decanoylamino-3-morpholino-1-propanol (PPMP), a potent and specific inhibitor of GCS, was shown to inhibit growth and encystation of giardia cells in culture (Hernandez *et al.* 2008; Sonda *et al.* 2008; Stefanic *et al.* 2010). Finally, both overexpression and knockdown of gGlcT1 disrupt viable cyst production (Mendez *et al.* 2013), and it appears that it is a balance of SL that is important because both increases and decreases in production lead to similar reductions in cyst formation. Taken together these data identify a clear requirement for SLs in order to complete the life cycle of *G. lamblia*.

1.5 Knowledge Gap and Aims of the Current Dissertation

The connection between gGlcT1 activity and encystation has been demonstrated, but it remains unclear whether this link is mediated by the enzyme itself, the lipid product, or both. In that same vein, although *Giardia* requires SLs and is to some extent able to modulate these molecules, it is not known if this represents a structural requirement, a signaling pathway, or both. The assumption that the majority of lipids are taken up from the environment can be reasonably extended to include SLs, but because Cer and SM uptake involves the cytoskeleton this is likely to be a regulated process that could potentially be selective. Early reports using thin-layer chromatography have suggested that the lipid profile of the growth media and *Giardia* trophozoites are similar, yet given the limitations of this technique it remains to be seen how "similar is similar"—i.e., are all classes of SLs found in the media represented in the *Giardia* profile, are the species of each class similar, and are there any classes/species of SL that are over or under-represented in the cell. A global SL profile, sphingolipidome, of *Giardia* has not been established conclusively and the ways that these lipids are modulated during encystation has not yet been established.

My dissertation focuses on characterizing the sphingolipidome of *Giardia* throughout its life cycle. I found that Cer and SM are the major SLs in this parasite and that their levels are altered during encystation. In addition, glycosphingolipids (GSLs), like monohexosyl-, dihexosyl-, and trihexosyl ceramides, are also present and elevated in encysting *Giardia*. Interestingly, viable cysts contain higher SM concentrations than non-viable cysts and efficiently undergo excystation *in vitro*. I also show that gASMLPD3b1 and gASMLPD3b2 are both functional and that over-expression of gASMLPD3b1 reduces *in vitro* excystation efficiency.

Chapter 2: Sphingolipidomics of *Giardia lamblia*

Sphingolipids (SLs) are both important structural components of plasma membranes and active signaling molecules implicated in cellular processes as varied as growth, differentiation, apoptosis, senescence and autophagy (Venable *et al.* 1995; Ogretmen and Hannun 2004; Scarlatti *et al.* 2004). Whereas early work has focused upon the role of entire classes of SLs in cellular processes and disease states, it is now increasingly recognized that for ceramide and SM there is evidence that each molecule is functionally distinct based upon both acyl chain length and degree of unsaturation (Ben-David and Futerman 2010; Grosch *et al.* 2012; Slotte 2013).

Metabolism of SLs occurs primarily in eukaryotes but has also been reported in some bacteria such as *sphingomonas spp* (Hannun and Obeid 2008). The synthesis of these lipids begins with the condensation of L-serine and palmitoyl-Coa (or myristate or stearate) to form 3-keto-sphinganine (3KS), which is subsequently reduced to sphinganine by 3-keto sphinganine reductase (3KSR) followed by acylation via either ceramide synthase or dihydroceramide synthase (Lass or CerS) to form dihydroceramide. Formation of Cer occurs upon desaturation of dihydroceramide. Once formed Cer becomes the backbone upon which complex SLs are formed. This is accomplished through glycosylation by glucosylceramide or galactosylceramide synthase (GlcT1/GCS), phosphorylation by ceramide kinase (CerK) or addition of a phosphocholine by SM synthase to form SM. The latter reaction produces diacylglycerol (DAG) from PC, highlighting the interconnected nature of SL metabolism and other lipid metabolic pathways.

Once formed, these lipids are broken down by specific hydrolases; Cer is produced through the hydrolysis of SM by SMase and glucosylceramide and galactosylceramide by specific β-glycosidases. Cleavage of the acyl chain from Cer produces sphingosine which can then be recycled for the formation of Cer or phosphorylated to sphingosine-1-phosphate. Exit from the SL pathway is carried out by sphingosine-1-phosphate, which is dephosphorylated by

sphingosine-phosphate phosphatase or irreversibly cleaved to ethanolamine and hexadecanal (Futerman and Riezman 2005; Hannun and Obeid 2008).

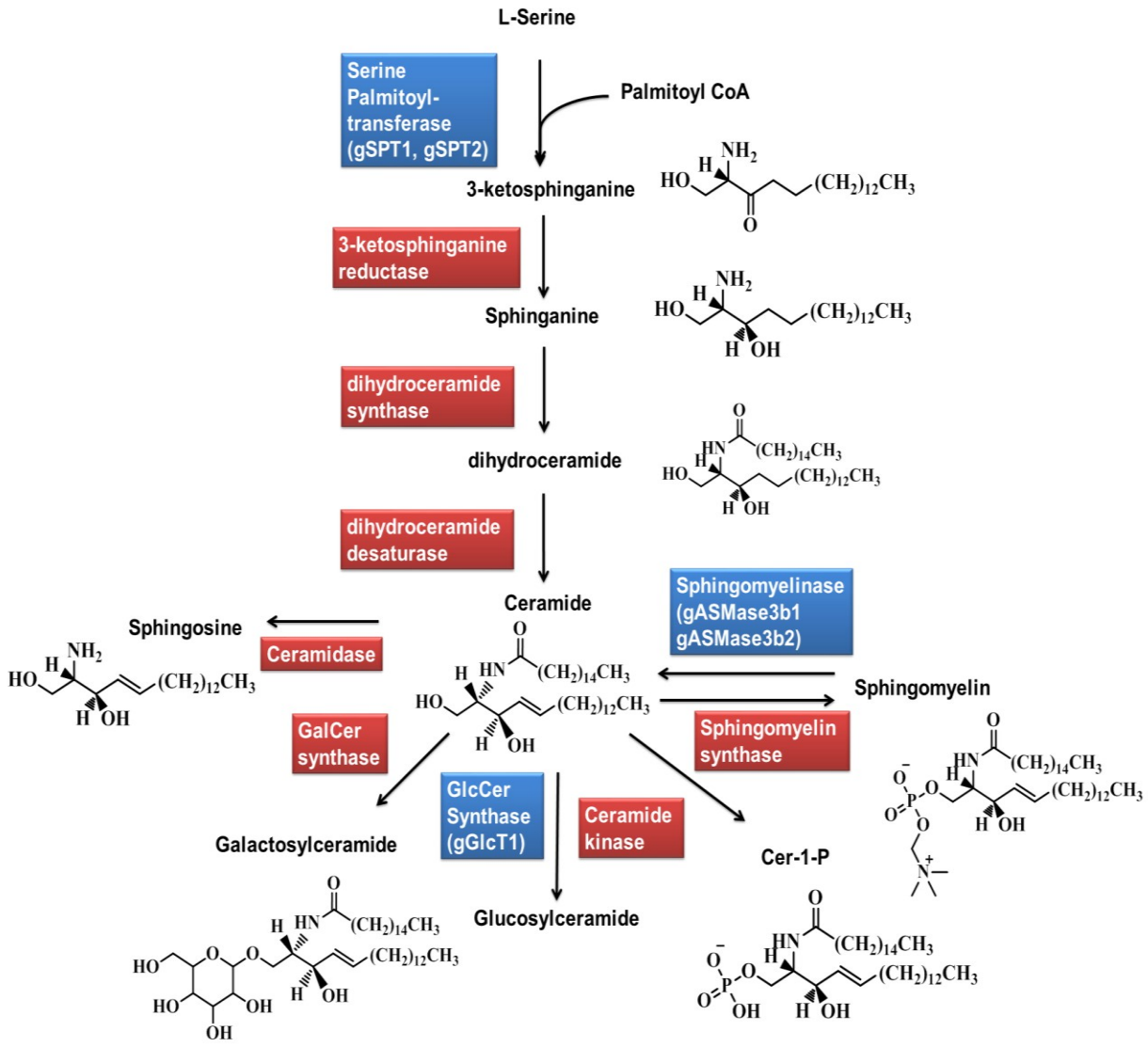

Figure 2.1: Sphingolipid metabolic pathway

SL enzymes are boxed; red boxes indicate enzymes not identified in *Giardia*, green boxes indicate those that were. Structures are representative, acyl chain and sphingoid base can vary in number of carbons.

As mentioned above, SL metabolism in *Giardia* is both fragmented and incomplete. In the genome database (www.giardiaDB.org) there are only five identified SL genes, and due to redundant pairs, there are only three SL metabolic functions. They are serine palmitoyltransferase (gSPT1 and gSPT2), sphingomyelinase (gASMLPD3b1 and gASMLPD3b2) and glucosylceramide synthase (gGlcT1). There are no apparent enzymes for the de-novo synthesis of sphingosine or Cer, nor are there any SL specific kinases capable of the formation of ceramide-1-phosphate or sphingosine-1-phosphate. However this does not preclude the possibility that these functions could be mediated through either a novel pathway or by enzymes with less than significant sequence similarity. Therefore, it is unclear the types of SLs that are present in *Giardia* and whether they are capable of synthesizing new SL molecules, or if SLs are simply scavenged from the environment. Based upon the assumption that *Giardia* has the ability to glycosylate Cer as well as generate Cer through hydrolysis of SM, I asked if the parasite was capable of other manipulations of these lipids not predicted by the genome. To approach this problem I performed a mass spectrometry based investigation into the SLs present in the cell as well as the media. I also investigated the presence/absence of SLs throughout the *Giardia* life cycle to identify stage specific regulation of these important molecules

2.1 MATERIALS AND METHODS

2.1.1 Materials

Unless otherwise specified, all chemicals were purchased from Sigma and were of the highest purity available. All solvents used for mass spectrometry were of LC/MS grade. Fluorescent (Bodipy- or NBD-conjugated) lipids were purchased from Invitrogen. N-palmitoyl-d31-D-erythro-sphingosine (deuterated ceramide) and N-palmitoyl-d31-D-erythro-sphingosylphosphorylcholine (deuterated sphingomyelin) as well as all other sphingolipid standards were obtained from Avanti Polar Lipids (Alabaster, AL). Sphingomyelin [choline methyl-14C] (bovine, 50-60 mCi/mmol) was purchased from American Radiolabeled Chemical (St. Louis, MO).

2.1.2 Parasite, encystation and excystation

Giardia lamblia trophozoites (assemblage A, strain WB C6), ATCC No. 30957) were cultivated following the method of Diamond et al. (Diamond *et al.* 1978) using modified TYI-S-33 medium supplemented with 10% adult bovine serum and 1% bovine bile (Keister 1983). The antibiotic piperacillin (100 μg/ml) was added during routine culturing of the parasite (Gillin *et al.* 1989). Trophozoites were detached from the culture flask by ice chilling and harvested by centrifugation at 1500 × g for 10 min at 4 °C, followed by three washings in sterile phosphate-buffered saline (PBS) and microscopic determination of cell numbers using a hemocytometer. *In- vitro* encystation was carried out by culturing the trophozoites in TYI-S-33 medium, pH 7.8, supplemented with adult bovine serum (10%, v/v), lactic acid (5 mM), and porcine bile (250 mg/ml) for various time points, as described previously (Gillin *et al.* 1989). Cells were allowed to encyst for 72 h, and cysts were isolated by centrifugation (2,500 × g for 10 min at 4 °C), washed three times in cold distilled water, and kept in water for 1 hour at 4°C. Isolated water-resistant cysts were counted or subjected to the microscopic experiments also described below. Excystation was carried out by two step method described previously (Boucher and Gillin 1990). Briefly, 2 x 10^6 cysts were exposed to strong acid for 1 h to mimic stomach conditions followed by culture in alkaline pH with trypsin to mimic conditions seen in the intestine. Cells were then allowed to recover in culture media and monitored for growth for 72 h in some experiments cells were counted after 72 hours.

2.1.3 Lipid Extraction

Cultured *Giardia* trophozoites (1x10^8cells) were harvested and transferred to 13 x150mm borosilicate glass tubes with polytetrafluoroethylene (PTFE) caps. These cells were washed twice with PBS and pelleted by centrifugation (1500 × g, 5 min). Cells were re-suspended in 1ml PBS and, following removal of 100uL aliquot for protein quantitation by Bradford assay, the remaining cells were lyophilized, flushed with N_2 and stored at -80 °C until extraction. This same procedure was carried out for cells 12 and 24 hours post induction of encystation (h.p.i).

Cysts were harvested after 72 h.p.i. then washed and re-suspended in cold distilled H_2O for 1 h prior to lyophilization. Lipids were also extracted from 1 ml bovine serum, bovine bile (52mg/ml) and porcine bile (50mg/ml) following the same extraction procedure. Each was lyophilized prior to extraction as with cell pellets. Freeze dried samples were re-suspended in MeOH to 1mg/mL protein. An aliquot equivalent to 1mg protein was removed to clean borosilicate glass tube and dried under N_2 stream. This was then resuspended in $CHCl_3$: MeOH (2:1,v,v) and incubated at 48 °C overnight. To remove possibly interfering glycerophospholipids, samples were treated with 100mM (final concentration) KOH for 2 hours at 37 °C. They were then allowed to cool to room temperature and pH was adjusted to 4-5 with glacial acetic acid (Sullards *et al.* 2007). Samples were centrifuged (900 x g, 5min) and supernatant was transferred to clean tube. SLs in the remaining pellet were then extracted twice with Isopropanol:Hexane:H_2O 55:25:20 v,v,v and finally with $CHCl_3$:MeOH 1:1 v,v (Li *et al.* 2008). Extracts were pooled and dried either under N_2 stream or in centrivap vacuum centrifuge.

2.1.4 Qualitative Lipidomics

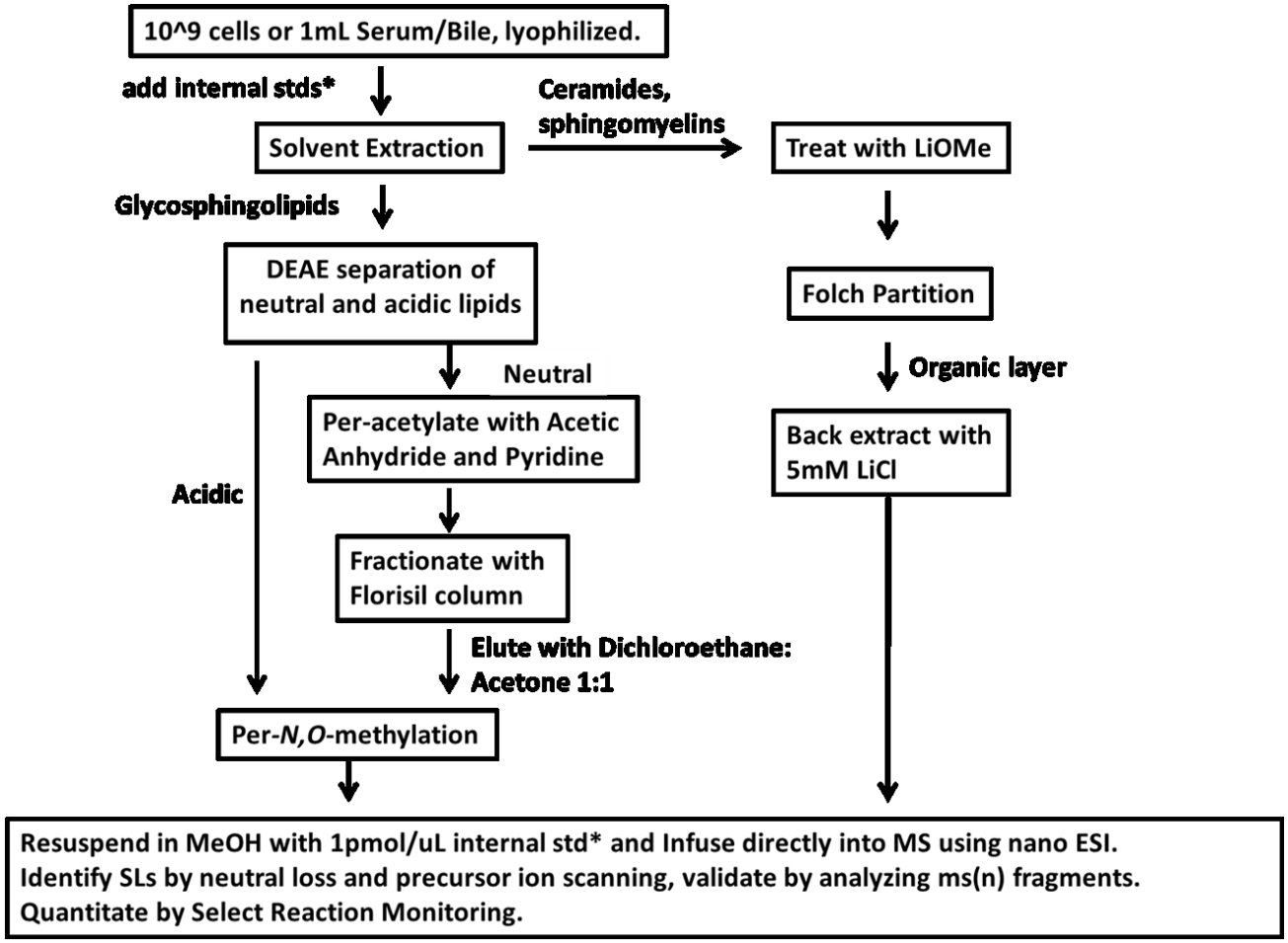

Figure 2.2: Flow chart for qualitative sphingolipidomics method

Glycosphingolipids

Separation of acidic and neutral GSLs and removal of non-GSL impurities from neutral glycosphingolipid fraction was carried out as described previously (Li *et al.* 2008) with the following modifications.

DEAE Chromatography

0.5g DEAE-Cl resin (Sigma-Aldrich) was swelled overnight in 10ml 0.5M NaOAc in $CHCl_3$:MeOH:H_2O 30:60:8 (lower phase.) Processed resin (1ml) was then packed onto a Pasteur pipette over a small amount of glass wool. The resin was washed with 10 bed volumes (10ml) $CHCl_3$:MeOH:H_2O (lower phase) and samples were loaded in the same solvent. Neutral lipids

were eluted with 5ml of the same solvent and acidic lipids were eluted with 5 ml of 0.8M NaOAc in MeOH. Eluates were dried as before, re-suspended in H_2O and desalted using a 3ml DSC-18 SPE cartridge (Supelco), dried and stored at -20 °C under N_2 until further processing. Neutral lipids were then per-N-acetylated with 4ml acetic anhydride and 2ml pyridine in the dark overnight then dried in centrivap.

Florisil Fractionation

To remove non-GSL impurities Florisil columns were prepared in Pasteur pipettes using a small amount of glass wool and 300mg of Florisil resin (60 mesh, Sigma-Aldrich). The resin was washed with 10ml dichloroethane (DCE):acetone 1:1 v,v, then 10ml DCE, and finally equilibrated with 10ml hexane:DCE 1:4 v,v. Samples were loaded in this solvent. Fraction F1 was eluted with 10ml hexane:DCE 1:4 v,v; Fraction F2 was eluted with 10ml DCE and Fraction F3, which is rich in GSLs, was eluted with DCE:acetone 1:1 v,v. Extracts were dried in centrivap and acetylated with 3ml 0.5N NaOMe in 6ml MeOH for 2 hours at room temperature. The reaction was stopped with 2ml 10% acetic acid in MeOH (pH 4-5) desalted as mentioned above, dried and stored under N_2 at -20 °C.

Per-N,O-Methylation of glycosphingolipids

Neutral GSL's from Florisil fraction F3 and acidic GSL's from DEAE eluate were methylated as described by Ciucanu and Kerek (Ciucanu 1984). Briefly GSLs were re-suspended in 150µL DMSO, 40-50 mg of NaOH was added and stirred until dissolved. The reaction was started by adding 80µl iodomethane and vortexed for 1h at room temperature. The reaction was quenched with 2ml H_2O and GSLs were then extracted with dichloromethane (DCM). Extracts were washed with H_2O, dried under N_2, re-suspended to 1mg/ml protein in MeOH and analyzed by nano-ESI mass spectrometry.

Sphingoid bases, sphingomyelins and ceramides

To identify SM species samples were extracted as described above. Extracts were partitioned by the Folch method (Folch et al. 1957). The lower chloroform phase was dried under N_2 and re-suspended in 500 µl MeOH and stored at -80 °C. An aliquot of this was removed for identification of Cer, the remainder was processed further for the identification of sphingoid bases and SM species. To ensure the complete removal of glycerophospholipids that could interfere with data interpretation (especially PC), samples were subjected to alkaline hydrolysis as described previously (Jiang *et al.* 2007). Briefly lipid extract was re-suspended in 200µl lithium methoxide in methanol (1M, Sigma-Aldrich), vortexed for 15 seconds then incubated at 0 °C for 1 h. Reaction was stopped with 0.4% glacial acetic acid (2ml), and pH was adjusted to 4-5. Aqueous solution was washed with 2ml hexane, then lipids were extracted by Folch partition. Lower chloroform phase was washed, with 50mM lithium chloride solution, dried under N_2, re-suspended in 500µl MeOH and stored at -80 °C until further analysis.

Ion Trap nano ESI MS/MS analysis

Analyses were carried out in positive ion mode on a linear triple quadrupole mass spectrometer (LTQ, thermo fisher). Samples were infused directly via Advion [Ithaca, NY] TriVersa NanoMate chip interface (capillary temperature 230°C), with injection time 100.00 ms, activation time 30 ms, activation Q-value, 0.250, isolation width m/z 2.0. Extracts from each fraction were diluted to 100fmols/µl protein equivalent and directly infused into the mass spectrometer. To improve ionization of samples that had not been methylated, 5mM LiOH was added. Full scans were recorded for ~1 minute in profile mode for each fraction in triplicate and Total Ion Mapping (TIM) was carried out over the mass range for analytes expected from each fraction. For ion mapping 3 µscans were taken with a mass interval of 2.0 and collision energy of 35kV. Ion mapping from each fraction was used to determine presence of SL species by looking for characteristic neutral loss or product ion masses. For example methylated

hexosylceramide species produce a characteristic product ion at m/z 258.6 corresponding to [methylated hexose +Na], dihexosylceramide produces a peak at 463.4 [(methylated hexose)$_2$ +Na], SM with a lithium adduct can be found with neutral loss of 59 [N(CH3)$_3$], for a complete list of TIM fragments used see Table 2.1 and 2.2. For structural validation, putative SL species identified from ion mapping were fragmented further (ms3 to ms5 depending on analyte abundance) to confirm sphingoid base and fatty acyl chain length. All files were acquired using Xcalibur software.

2.1.5 Sphingolipid Quantitation

Due to the high concentration of SM in *Giardia* extracts, SLs extracted above were separated as described previously (Pernet *et al.* 2006) off-line, prior to on-line HPLC. Briefly, ~200 mg Silica gel (60A, Sigma-Aldrich) was poured into a Pasteur pipette, washed with 10ml MeOH followed by 10ml of acetone before equilibrating with 10ml CHCL$_3$. Samples equivalent

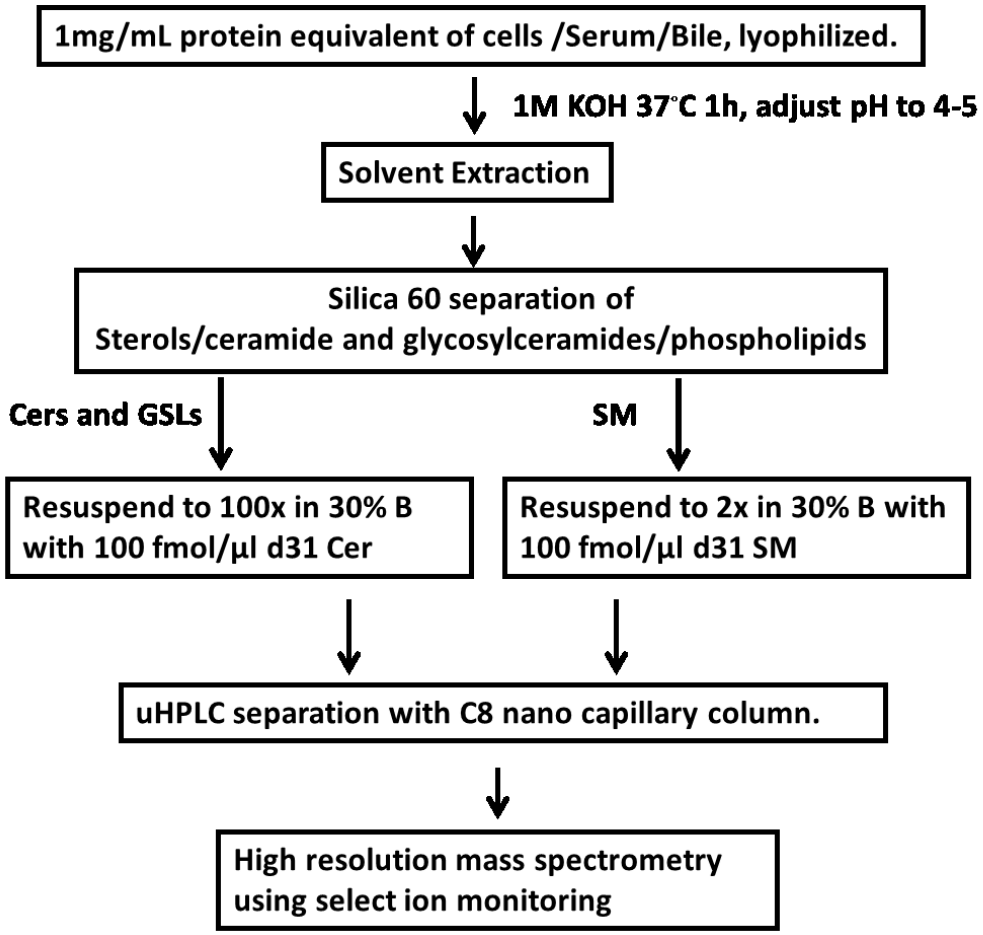

Figure 2.3: Flow chart with quantitative sphingolipidomics methods

to 1mg of protein were loaded onto column in 1mL $CHCl_3$. Neutral lipids (hydrocarbons, sterols) were eluted with 10ml $CHCl_3$, followed by glycolipids and ceramides with 10ml of acetone and finally phospholipids were eluted with 10ml MeOH. All fractions were dried under N_2 then re-suspended in methanol to an equivalent of 100fmol/µl protein and stored at -80 °C until further use.

HPLC

Reverse phase high pressure liquid chromatography (HPLC) was performed using a nano-capillary column, slurry packed in the laboratory (0.075mm x 100mm, C8 resin 3µm beads Pinnacle II Restek Corp.). Solvent A: 30:70 acetonitrile:H_2O with 10mM ammonium formate

and 0.2% formic acid. Solvent B: 90:10 isopropanol: acetonitrile with 10mM ammonium formate and 0.02% formic acid. Sample (1 µl) (100fmol protein equivalent) was spiked with 100fmol deuterated d18:1/16:0 SM (d31) and 100 fmol deuterated d18:1/16:0 Cer (d31) then loaded onto column in 70/30 A/B. Gradient began at 30%B for 10 minutes followed by a ramp from 30% B to 80%B over 5 minutes, plateaued at 80%B for 2minutes, then ramp from 80%B to 99%B over 25minutes. This was followed by 10 minutes at 99%B then a return to starting conditions over 5minutes and equilibration for an additional 38 minutes.

Fourier Transform nano ESI MS/MS

Samples were analyzed by high resolution mass spectrometry (QExactive, Thermo Fisher). Data were collected by select ion monitoring (SIM) with resolution of 70,000 as well as targeted ms2 (tMS2) with resolution of 35,000 from inclusion list containing species identified previously (see qualitative mass spectrometry above). SIM chromatograms were filtered for exact mass of species of interest and peak detection and integration were performed using Xcalibur v2.1 processing software (ISCIS detection, mass tolerance 5ppm, smoothing 7, baseline window 40, area noise factor 10, peak noise factor 20, minimum peak height S/N 3). Integrated peak areas were divided by integrated area of internal standard peak (D_{31} d18:1/16:0 Cer for ceramides and glycosphingolipids and D_{31} d18:1/16:0 SM for SM species) and response ratio was plotted on linear calibration curves to give absolute concentration of SL. Curves were generated by LC MS/MS using increasing concentrations of standards while maintaining 100fmol/µl D_{31} Cer or D_{31} SM followed by peak integration, calculation of response ratio and linear regression. I found that response ratios vs. D_{31} Cer under these conditions for medium to long chain ceramide, glucosylceramide and lactosylceramide were very similar and therefore all were plotted together to generate linear equation used for the calculations of these species. SM curve was constructed separately. Each sample was run in triplicate and the result recorded as mean plus standard error (n=3). Each species was confirmed by analyses of simultaneous tMS2

to identify characteristic fragment peaks (264.2686 and 266.2842 for d18:1 and d18:0 sphingoid bases respectively as well as 184.0733 for SM choline). Final result was given as pmol/cell using protein standard curves generated from 10^4, 10^5, 10^6 and 10^7 cells.

2.1.6 Statistical Analyses

All results are given as mean ± SE (n=3), and statistical analyses were generated using Sigma Plot software version 12.0 (Systat Software Inc. San Jose, CA). In all experiments student t-tests were performed and statistical values less than 0.05 were considered significant.

2.2 RESULTS

2.2.1 Shotgun sphingolipidomic analysis

The process of encystation and cyst formation is critical for the survival of *Giardia* outside of the host intestine. Previously we have shown that the modulation of glucosylceramide influences the biogenesis of ESVs and cyst viability, indicating that glucosylceramide and other SLs play important role for proper cyst formation. Interestingly, the SL metabolic pathway in *Giardia* is limited to two copies of serine palmitoyltransferase (gSPT1 and gSPT2), two copies of a sphingomyelinase like phosphodiesterase (gASMLPD3b1 and gASMLPD3b2) and a single copy of glucosylceramide transferase-1 (gGlcT1) (Hernandez *et al.* 2008). Given this incomplete and disjointed pathway we thought it likely that SLs were being taken up from sources within the culture media (specifically bovine serum). However it was not known how these lipids would be manipulated by the parasite or the fate of scavenged lipid during the process of encystation and cyst formation. To investigate this, we conducted shotgun sphingolipidomics by direct infusion via chip based nano-ESI on a linear triple quadrupole ion trap mass spectrometer (LTQ Thermo Fisher).

Infused samples were subjected to total ion mapping and then queried for characteristic ion fragments i.e. neutral loss or parent daughter mass transitions. We found that per-*N,O*-methylated GSL species could be readily identified by a predominant glycan peak (figure 2.4-

2.5, Table 2.1 and 2.2). Per-*N,O*-methylated ceramide could be distinguished by neutral loss of 48 Da as well as a prominent peak at 278.6 (for d18:1 sphingoid base containing species). Interestingly, on our instrument under these conditions we found that fragmentation of lithiated Cer (not methylated) which generate a well characterized peak at 264.2 did not yield many species. Perhaps due to the low abundance of these, we found that per-*N,O*-methylation of Cer greatly increased the number of species we could identify. SM in the presence of 5mM LiOH was identified by a neutral loss of 59 Da.

.

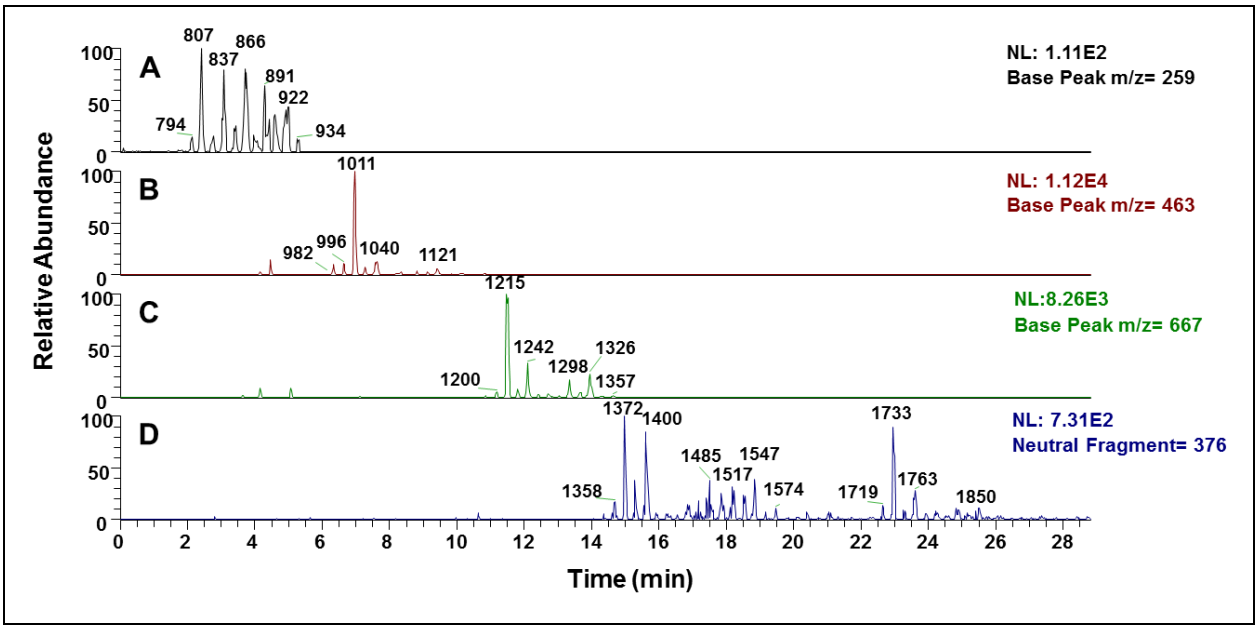

Figure 2.4: Total Ion Map of *Giardia lamblia* SL extracts

A, B, C. per-*N,O*-methylated Florisil Fraction 3 filtered for 259 (Hexose+Na), 463 ($Hexose_2$ +Na) and 667 ($Hexose_3$ +Na) respectively. D. DEAE acid fraction filtered for Neutral fragment of 376 Daltons (Sialic acid).

Further characterization and confirmation was carried out by analyzing ms(n) fragmentation following the in-depth studies reviewed by Levery, for GSLs (Levery 2005) as well as Hsu and Turk's work with lithiated SM (Hsu and Turk 2000). We identified ceramide,

hexosylceramide, dihexosylceramide, trihexosylceramide, SM, HexNAc-trihexosylceramide and HexNAc-tetrahexosylceramide among neutral SLs (please see Table 2.1 and 2.2 for species and mass filters). The majority of these species consisted of d18:1 sphingosine backbones and acyl chains ranging from C14 to C24. Acidic species identified were d18:1/C14-C24 GM3 (mono-sialo dihexosylceramide, d18:1/C14-C24 GD3 (di-sialo dihexosylceramide) and d18:1/16:0 and d18:1/18:0 GM1 (mono-sialo HexNAc trihexosylceramide). Extracts from trophozoites, 12 h.p.i, 24 h.p.i, cysts and bovine serum all showed similar profiles. From extracts of bovine bile as well as well as porcine bile we identified Cer and SM species but no GSLs were found in these samples. Given the lack of Cer synthase and SM synthase in the Giardia genome database (www.giardiadb.org), our analyses indicate that the majority of these SLs are scavenged from the culture media by trophozoites

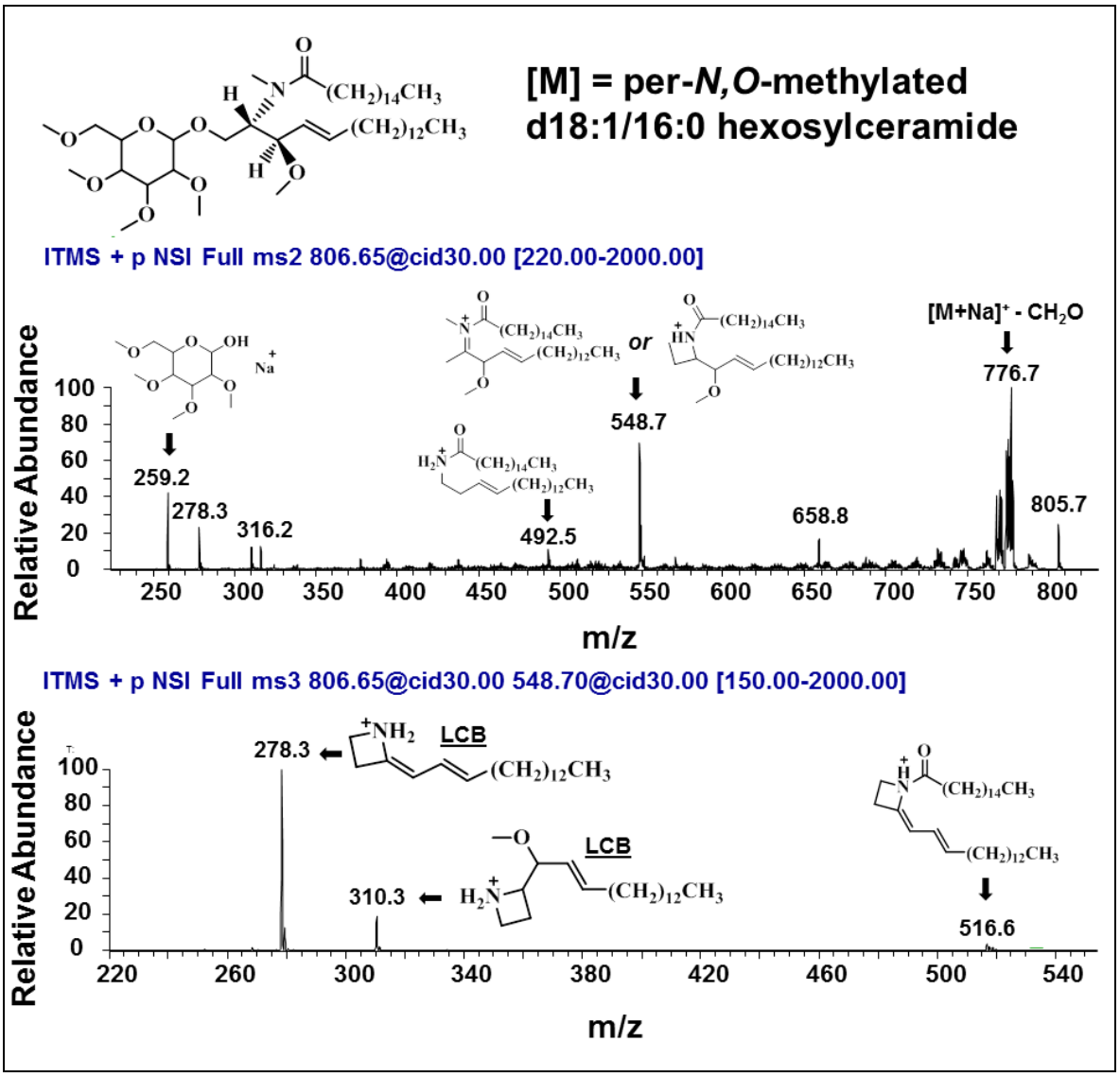

Figure 2.5: Representative fragmentation analysis of a neutral glycosphingolipid

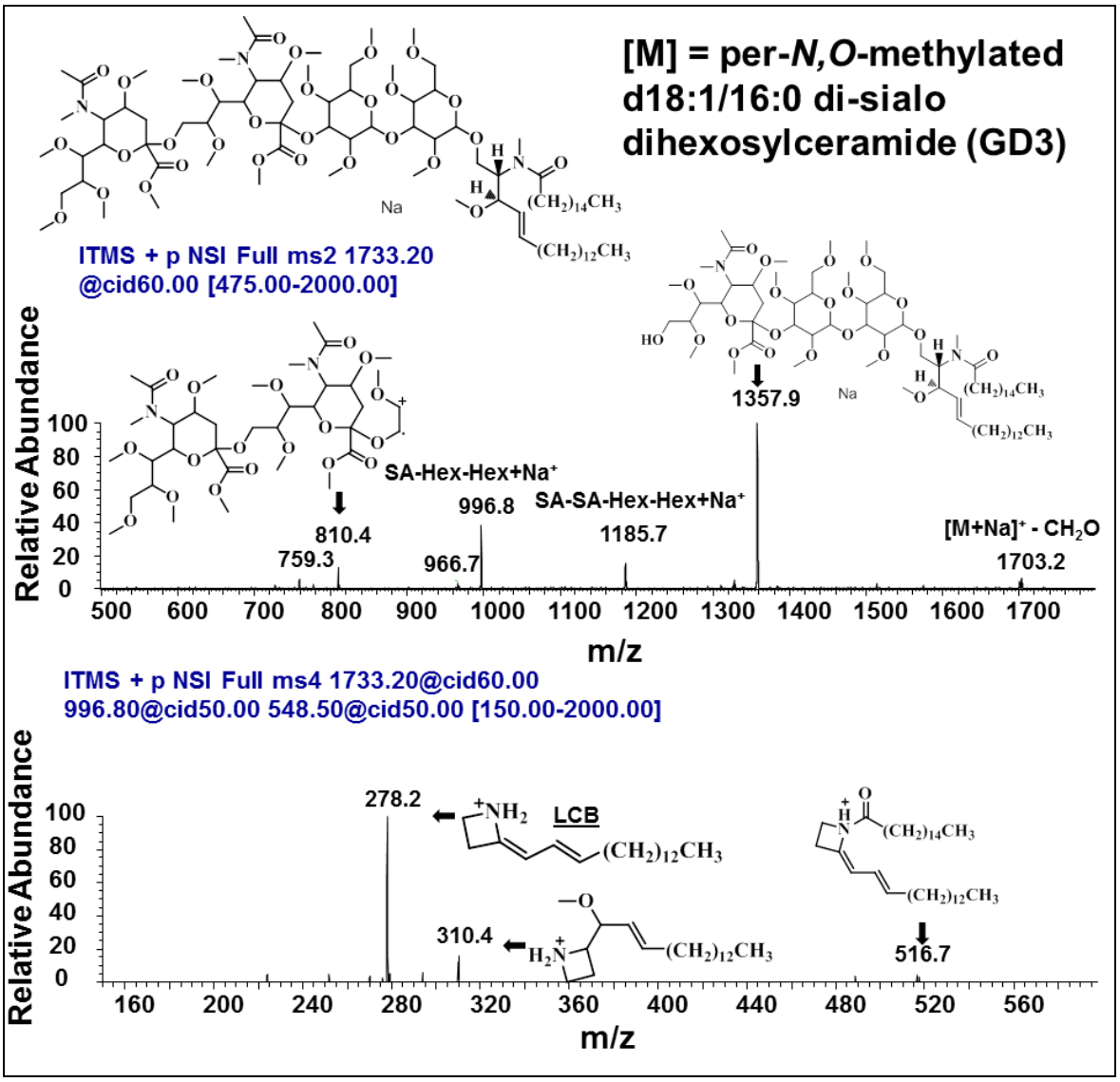

Figure 2.6: Representative fragmentation analysis of an acidic glycosphingolipid

Table 2.1 Acidic sphingolipids identified in this study:

Sphingolipid Species	$[M+Na]^+$	TIM Filter
d18:1/26:0 GM3	1512	NL 376
d18:1/25:0 GM3	1498	NL 376
d18:1/24:0 GM3	1484	NL 376
d18:1/23:0 GM3	1470.8	NL 376
d18:1/22:0 GM3	1456.8	NL 376
d18:1/21:0 GM3	1442.8	NL 376
d18:1/20:0 GM3	1428.8	NL 376
d18:1/19:0 GM3	1414.8	NL 376
d18:1/18:0 GM3	1400.8	NL 376
d18:1/18:1 GM3	1398.8	NL 376
d18:1/17:0 GM3	1386.8	NL 376
d18:1/17:1 GM3	1384.8	NL 376
d18:1/16:0 GM3	1372.8	NL 376
d18:1/16:1 GM3	1370.8	NL 376
d18:1/15:0 GM3	1358.8	NL 376
d18:1/14:0 GM3	1344.8	NL 376
d18:1/26:0 Gd3	1874	NL 376
d18:1/25:0 Gd3	1860	NL 376
d18:1/24:0 Gd3	1846	NL 376
d18:1/23:0 Gd3	1832	NL 376
d18:1/22:0 Gd3	1818	NL 376
d18:1/21:0 Gd3	1804	NL 376
d18:1/20:0 Gd3	1790	NL 376
d18:1/19:0 Gd3	1776	NL 376
d18:1/18:0 Gd3	1762.19	NL 376
d18:1/17:0 Gd3	1748.19	NL 376
d18:1/16:0 Gd3	1734.19	NL 376
d18:1/15:0 Gd3	1720.19	NL 376

d18:1/16:0 GM1	1822	BP 1273
d18:1/18:0 GM1	1850	BP 1273

Table 2.2 Neutral sphingolipids identified in this study

Sphingolipid Species	$[M+Na]^+$	TIM Filter
D18:1/26:0 HexNAc-(Hexose)3-Cer	1590.0	NL 260
D18:1/25:0 HexNAc-(Hexose)3-Cer	1586.0	NL 260
D18:1/24:0 HexNAc-(Hexose)3-Cer	1572.0	NL 260
D18:1/23:0 HexNAc-(Hexose)3-Cer	1558.0	NL 260
D18:1/22:0 HexNAc-(Hexose)3-Cer	1544.0	NL 260
d18:1/21:0 HexNAc-(Hexose)3-Cer	1530.0	NL 260
d18:1/20:0 HexNAc-(Hexose)3-Cer	1516.0	NL 260
d18:1/19:0 HexNAc-(Hexose)3-Cer	1502.0	NL 260
d18:1/18:0 HexNAc-(Hexose)3-Cer	1488.0	NL 260
d18:1/17:0 HexNAc-(Hexose)3-Cer	1474.0	NL 260
d18:1/16:0 HexNAc-(Hexose)3-Cer	1460.0	NL 260
d18:1/15:0 HexNAc-(Hexose)3-Cer	1446.0	NL 260
d18:1/24:0 Hexose-HexNAc-(Hexose)3-Cer	1734.0	NL260
d18:1/20:0 Hexose-HexNAc-(Hexose)3-Cer	1706.0	NL260
d18:1/18:0 Hexose-HexNAc-(Hexose)3-Cer	1678.0	NL260
d18:1/16:0 Hexose-HexNAc-(Hexose)3-Cer	1650.0	NL260
d18:1/14:0 trihexosylceramide	1186.0	BP 667
d18:1/15:0 trihexosylceramide	1200.0	BP 667
d18:1/16:0 trihexosylceramide	1214.0	BP 667
d18:1/17:0 trihexosylceramide	1228.0	BP 667
d18:1/18:0 trihexosylceramide	1242.0	BP 667
d18:1/19:0 trihexosylceramide	1256.0	BP 667
d18:1/20:0 trihexosylceramide	1270.0	BP 667

d18:1/21:0 trihexosylceramide	1284.0	BP 667
d18:1/22:0 trihexosylceramide	1298.0	BP 667
d18:1/23:0 trihexosylceramide	1312.0	BP 667
d18:1/24:0 trihexosylceramide	1326.0	BP 667
d18:1/25:0 trihexosylceramide	1340.0	BP 667
d18:1/26:0 trihexosylceramide	1354.0	BP 667
d18:1/14:0 dihexosylceramide	982.7	BP 463
d18:1/15:0 dihexosylceramide	996.7	BP 463
d18:1/16:1 dihexosylceramide	1008.6	BP 463
d18:1/16:0 dihexosylceramide	1010.7	BP 463
d18:1/17:0 dihexosylceramide	1024.8	BP 463
d18:1/18:0 dihexosylceramide	1038.8	BP 463
d18:1/19:0 dihexosylceramide	1052.8	BP 463
d18:1/20:0 dihexosylceramide	1066.8	BP 463
d18:1/22:0 dihexosylceramide	1094.8	BP 463
d18:1/23:0 dihexosylceramide	1108.9	BP 463
d18:1/24:1 dihexosylceramide	1120.9	BP 463
d18:1/24:0 dihexosylceramide	1122.9	BP 463
d18:1/14:0 Hexosylceramide	778.6	BP 259
d18:1/15:0 Hexosylceramide	792.6	BP 259
d18:1/16:0 Hexosylceramide	806.6	BP 259
d18:1/17:0 Hexosylceramide	820.7	BP 259
d18:1/18:0 Hexosylceramide	834.7	BP 259
d18:1/19:0 Hexosylceramide	848.6	BP 259
d18:1/20:0 Hexosylceramide	862.6	BP 259
d18:1/21:0 Hexosylceramide	876.6	BP 259
d18:1/22:0 Hexosylceramide	890.6	BP 259
d18:1/23:0 Hexosylceramide	904.6	BP 259
d18:1/24:1 Hexosylceramide	916.8	BP 259
d18:1/24:0 Hexosylceramide	918.8	BP 259
d18:1/14:0 Ceramide	574.5	NL 30

d18:1/15:0 Ceramide	588.5	NL 30
d18:1/16:0 Ceramide	602.5	NL 30
d18:1/17:0 Ceramide	616.6	NL 30
d18:1/18:0 Ceramide	630.6	NL 30
d18:1/19:0 Ceramide	644.6	NL 30
d18:1/20:0 Ceramide	658.6	NL 30
d18:1/22:0 Ceramide	686.6	NL 30
d18:1/23:0 Ceramide	700.7	NL 30
d18:1/24:1 Ceramide	712.7	NL 30
d18:1/24:0 Ceramide	714.7	NL 30
	$[M+Li]^+$	
d18:1/15:0 sphingomyelin	695.6	NL 59
d18:1/16:0 sphingomyelin	709.6	NL 59
d18:1/17:0 sphingomyelin	723.6	NL 59
d18:1/18:0 sphingomyelin	737.6	NL 59
d18:1/19:0 sphingomyelin	751.6	NL 59
d18:1/20:0 sphingomyelin	765.6	NL 59
d18:1/22:0 sphingomyelin	793.7	NL 59
d18:1/23:1 sphingomyelin	805.6	NL 59
d18:1/23:0 sphingomyelin	807.7	NL 59
d18:1/24:1 sphingomyelin	819.7	NL 59
d18:1/24:0 sphingomyelin	821.7	NL 59
d18:1/26:0 sphingomyelin	849.7	NL 59

2.2.2 Quantitation of Sphingolipids

The limitation of our exploratory approach (described above) by direct infusion is the inability to quantitate the abundance of each species. This is due in part to ion suppression, which can be very high in these complex mixtures, as well as the failure to differentiate isobaric species. Furthermore, incomplete per-*N,O*-methylation could potentially inflate the number of species identified. To bypass this, we analyzed neutral sphingolipids by tandem nano HPLC-

MS/MS on a bench top orbitrap mass spectrometer (QExactive, Thermo fisher). Due to large differences in SM concentration vs. Cer and GSL abundance, samples were separated off-line using a silica 60 column prepared in a Pasteur pipette as described in 2.1.5. After verifying individual SLs by retention time and targeted MS-2 fragmentation (Fig 2.7), Select Ion Monitoring (SIM) scans were used for quantitation (Fig 2.8).

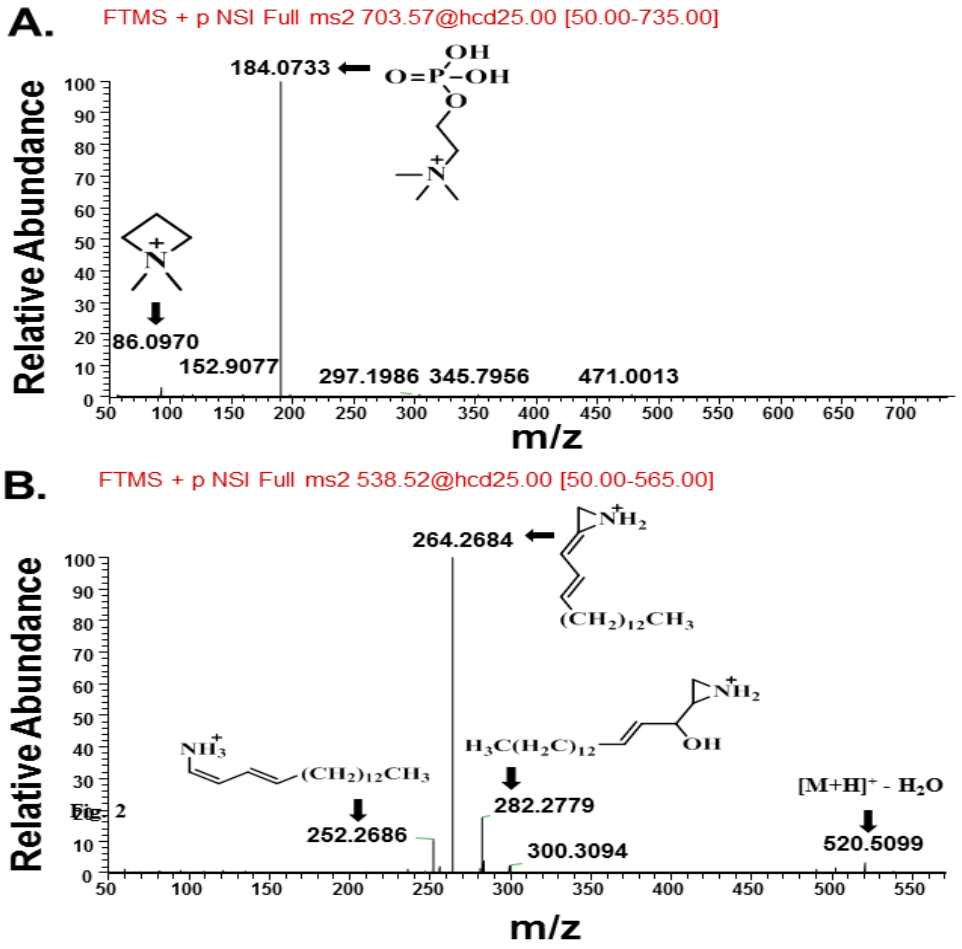

Figure 2.7: Identification of sphingolipids for quantitation by fragmentation and exact mass

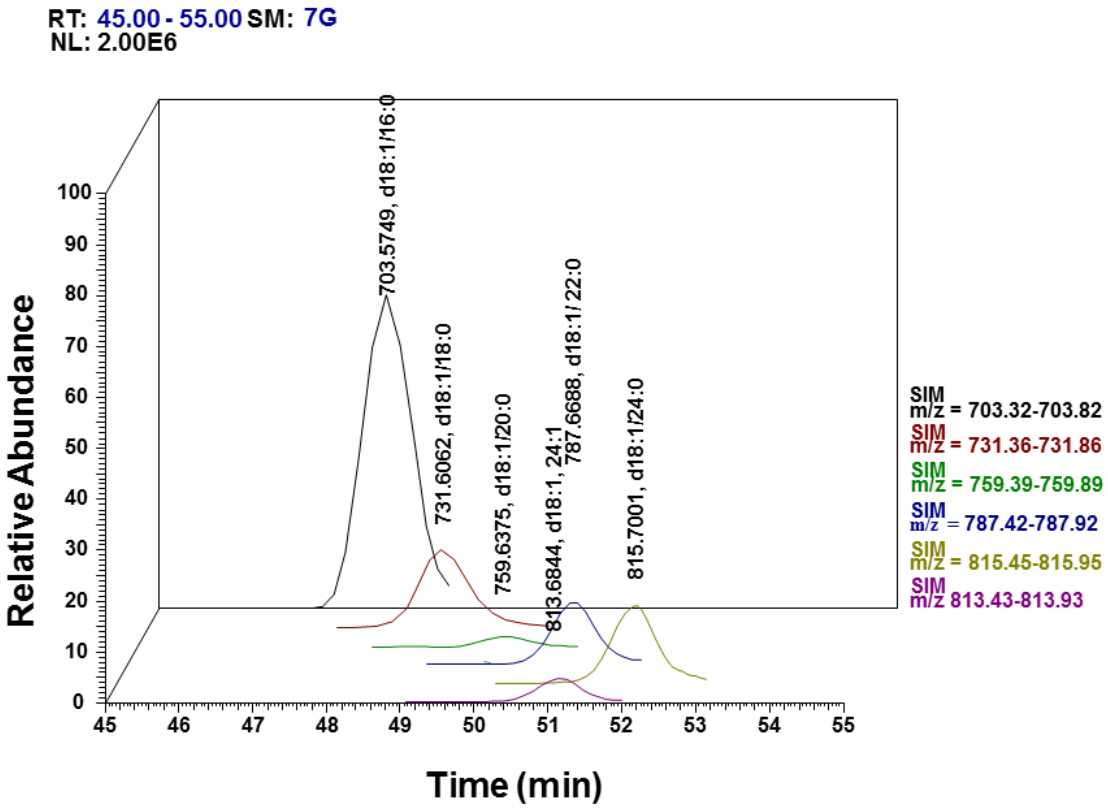

Figure 2.8: Representative extracted ion chromatograms used for SIM.

Calibration curves were generated to ensure that this method is linear and efficiently identifies the ionization differences. We found that carbon chain length in the standards analyzed had little effect on the response ratio to internal standard. Furthermore, response ratios for ceramides and glycosylceramides were similar enough to plot all data on a single graph (Fig. 2.9) To quantitate respective lipids, the integrated area of extracted ion chromatograms for each SIM reaction was divided by the integrated area of the extracted ion chromatogram for a stable isotope labeled internal standard (D_{31} d18:1/16:0 SM for SM samples, D_{31} d18:1/16:0 Cer for ceramides and glycosylceramides) to generate a response ratio using the processing software in Xcalibur v2.1. Concentrations were calculated from these response ratios using linear equations generated from calibration curves. This method allowed us to analyze SL extracts from trophozoites, two time points during encystation (12 and 24 h.p.i.) and cysts. Further

quantitation was performed for the culture media sources of SLs (bovine bile and bovine serum) and the encysting media sources of SLs (bovine serum and porcine bile).

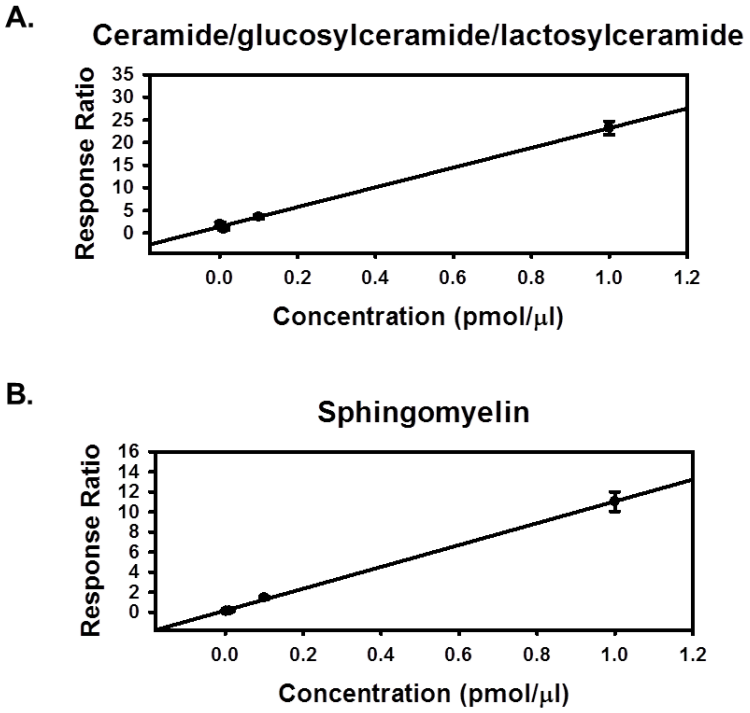

Figure 2.9: Calibration curves used for quantitation of SLs

LC-MS/MS high resolution mass spectrometry in both Select Ion Monitoring and ms2 modes allowed us to identify two other much less abundant sphingoid bases, d18:0 and d18:2. Further differences included identification of GSLs in both bovine and porcine bile as well as longer chain fatty acids, including C25 and C26 in all samples. This method, however, failed to identify the HexNAc containing GSLs. This could be due to differences in extraction procedures between the two methods used in the current study.

2.2.3 Neutral SLs are Abundant in Encysting *Giardia*

Although the overall SL profile remained mostly unchanged during encystation the proportion of each species (sphingoid base/acyl chain combination in each class) of lipid differed between the cell and the media that cell was grown in (Fig. 2.10-2.14). Based upon the

assumption that passive uptake would lead to identical profiles between cell and media, this observation indicates either selective uptake from the media or evidence of the parasites ability to modify these lipids once they have been scavenged from the culture environment.

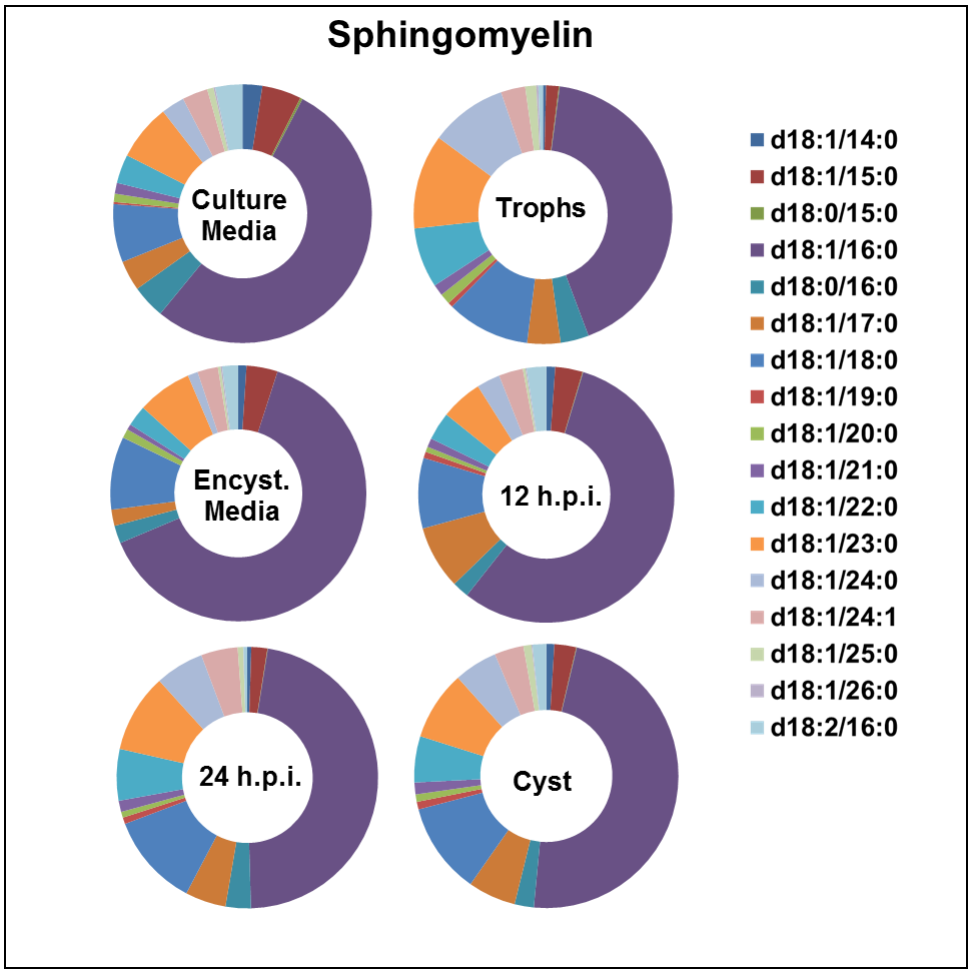

Figure 2.10: Percent composition of sphingomyelin

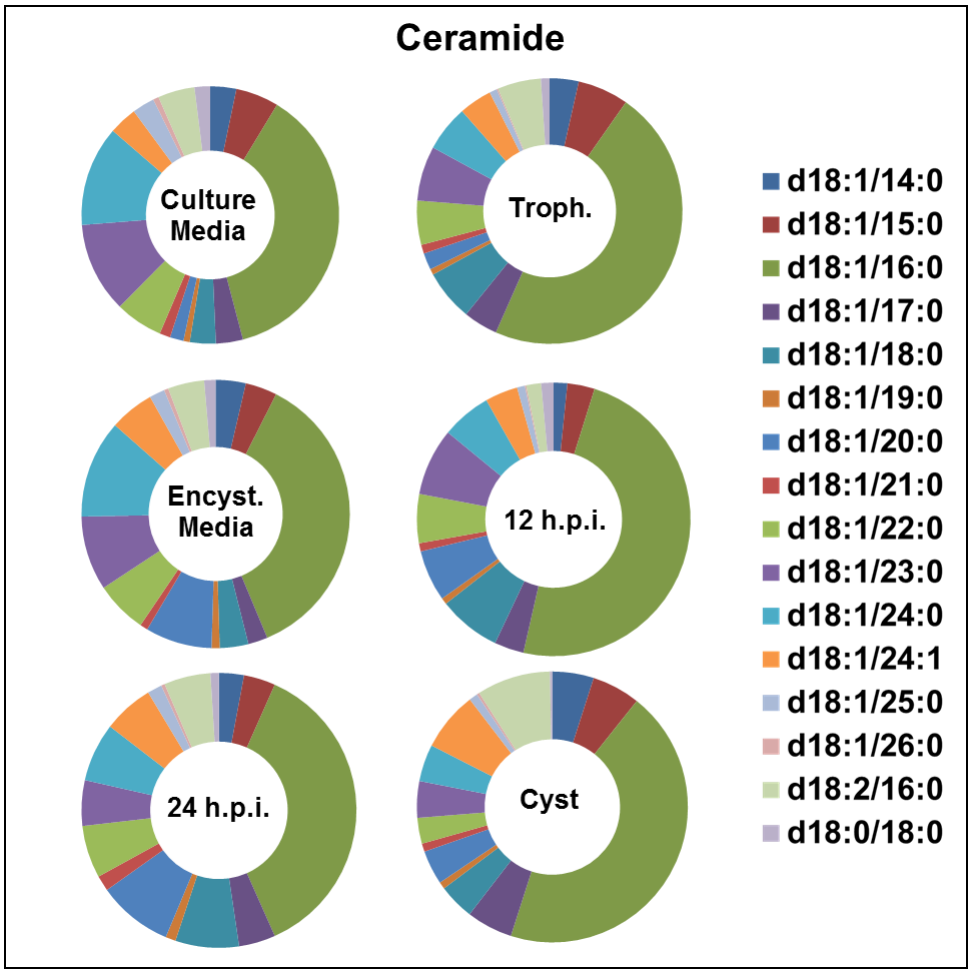

Figure 2.11: Percent composition of ceramide

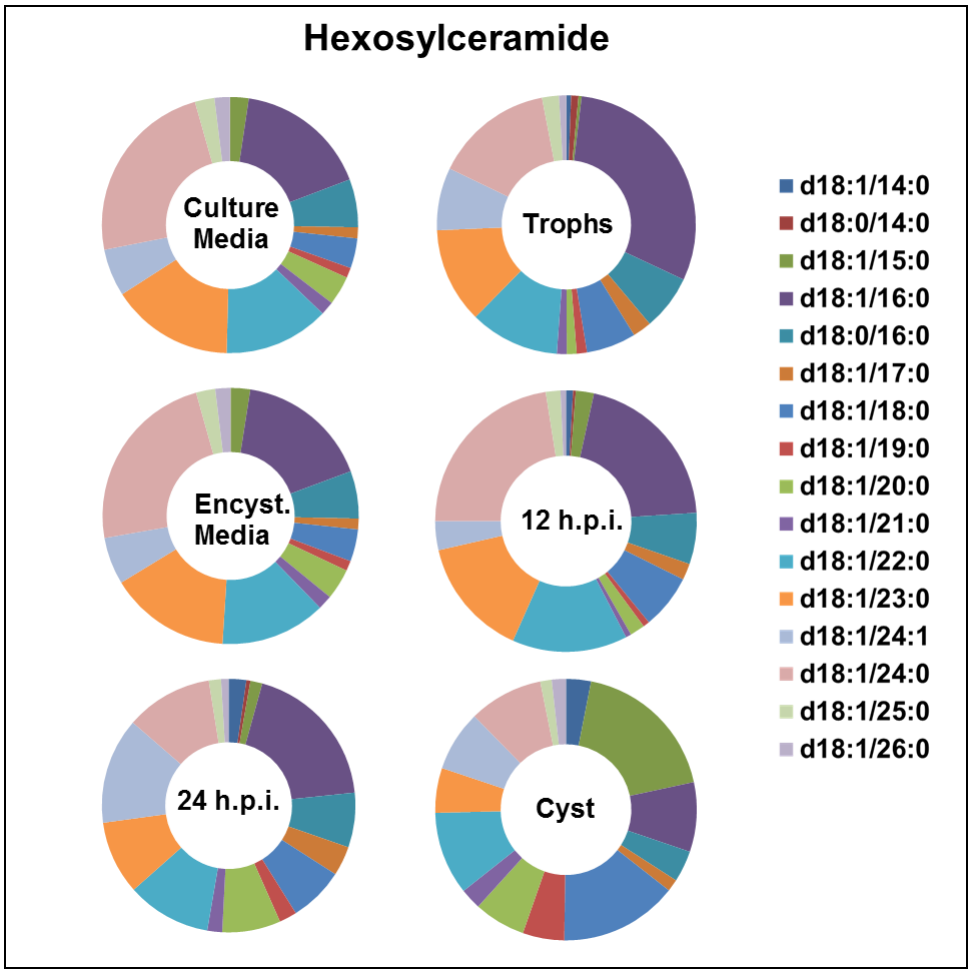

Figure 2.12: Percent composition of hexosylceramide

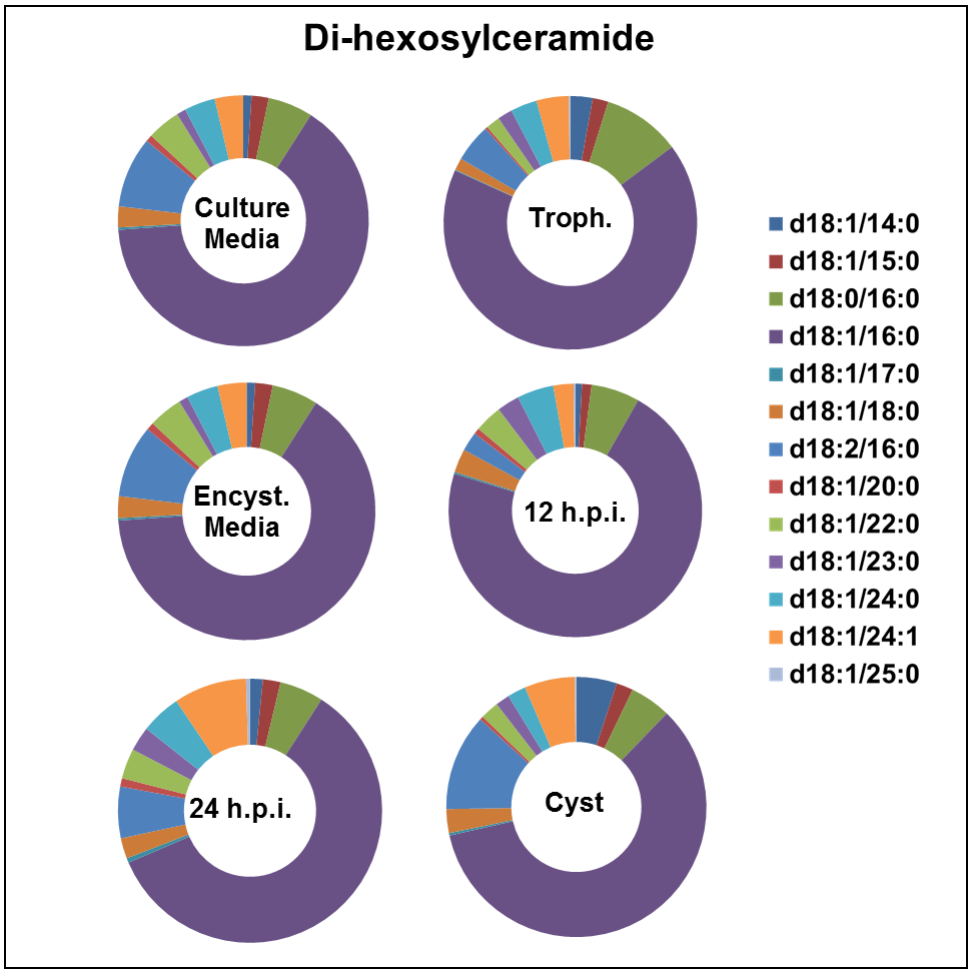

Figure 2.13: Percent composition of dihexosylceramide

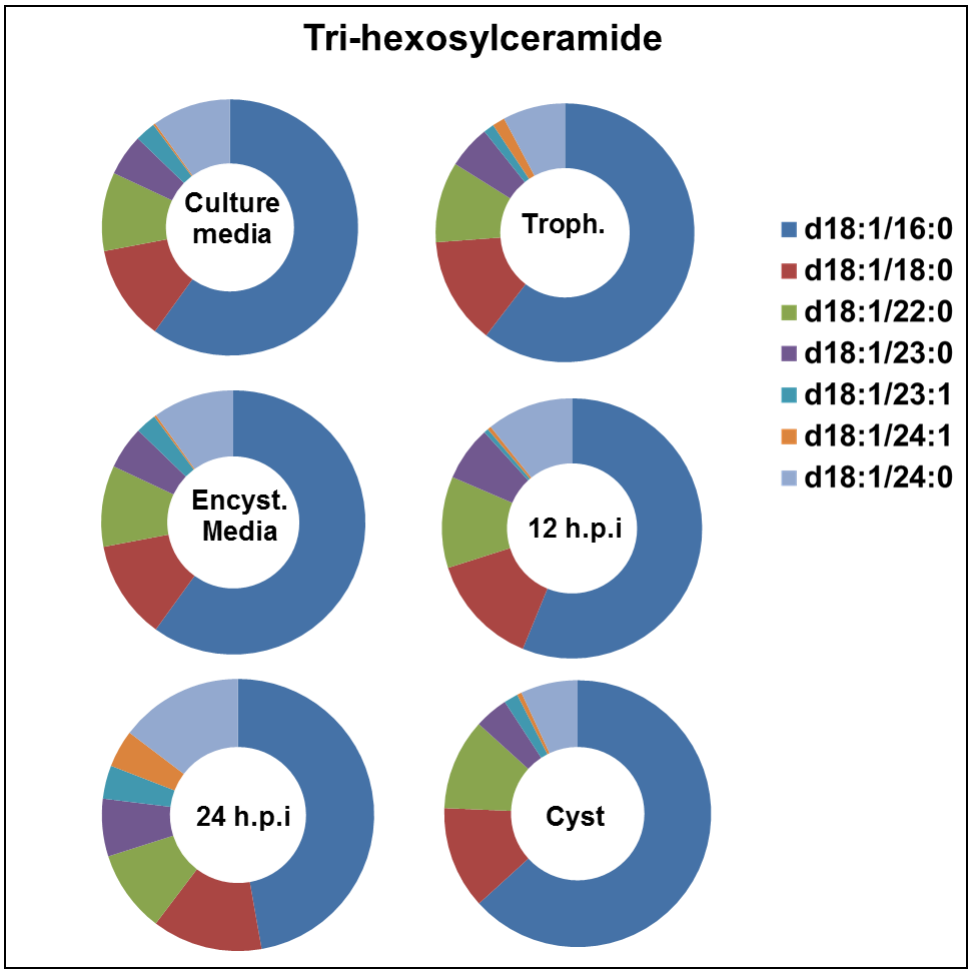

Figure 2.14: Percent composition of trihexosylceramide

To investigate changes in SLs by class, I used the total abundance given by the sum of the species in that class for each time point analyzed. I found that the levels of Cer and GSLs all increase during cyst formation. Within 24 h.p.i., Cer increases 10 fold; hexosylceramide, dihexosylceramide and trihexosylceramide increase between 11 and 12 fold. (Fig 2.15A and 2.15C). Each of these then decrease in cysts although remain slightly above trophozoite levels. Interestingly, total SM decreases 5 fold by 12 h and then increases, with cyst levels 3 fold greater than trophozoites (Fig. 2.15B). When these data are normalized by protein concentration this increase is greater than 40 fold (not shown), however due to changes in protein concentration throughout encystation I believe that normalization per cell more accurately reflects SL abundance in each stage. This increase of SM in the cyst form of the parasite is unexpected and

requires further investigation. Changes in individual lipid species relative to trophozoites are shown by heat mapping (Fig 2.16).

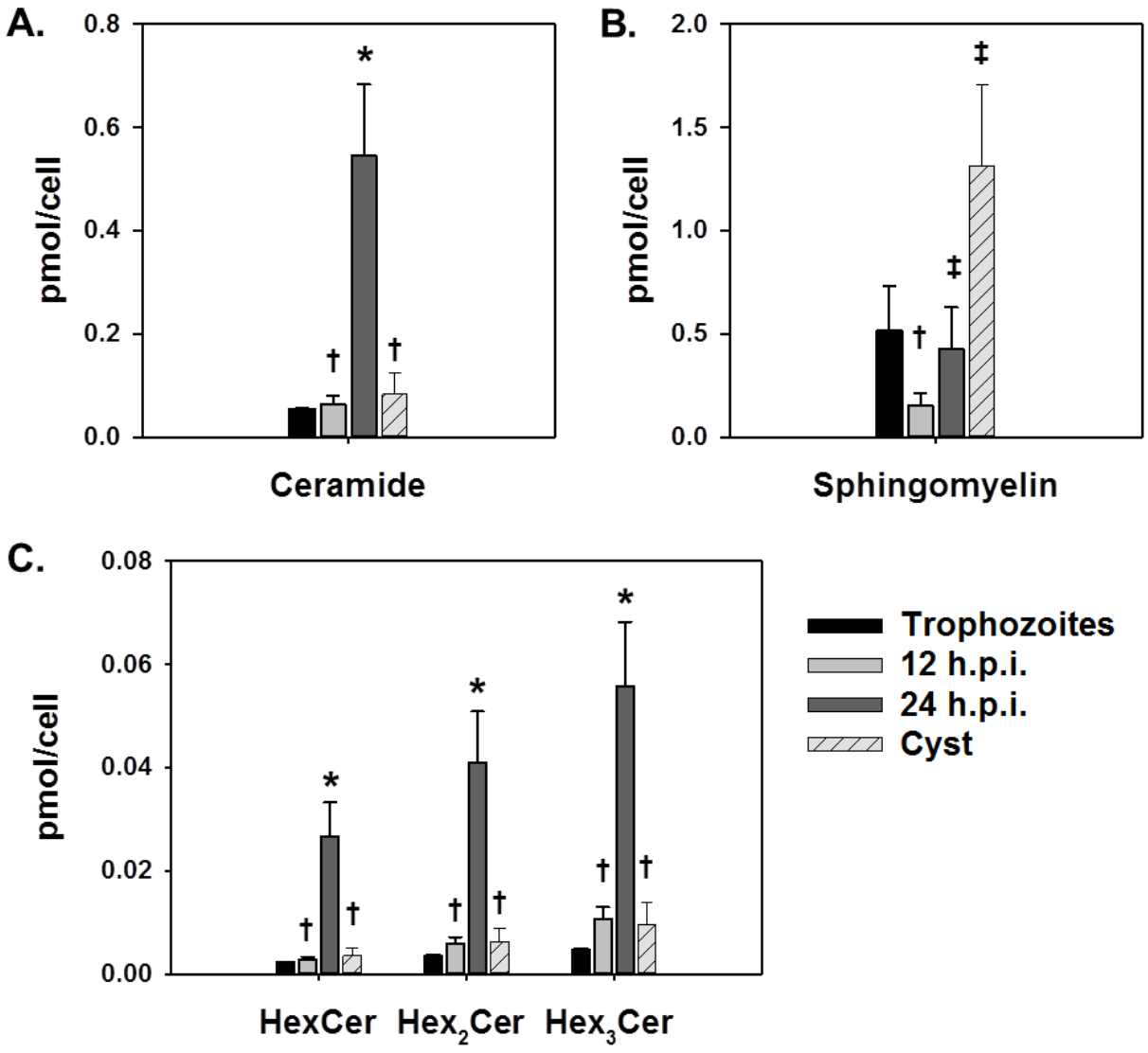

Figure 2.15: Comparison of total SL abundance during encystation

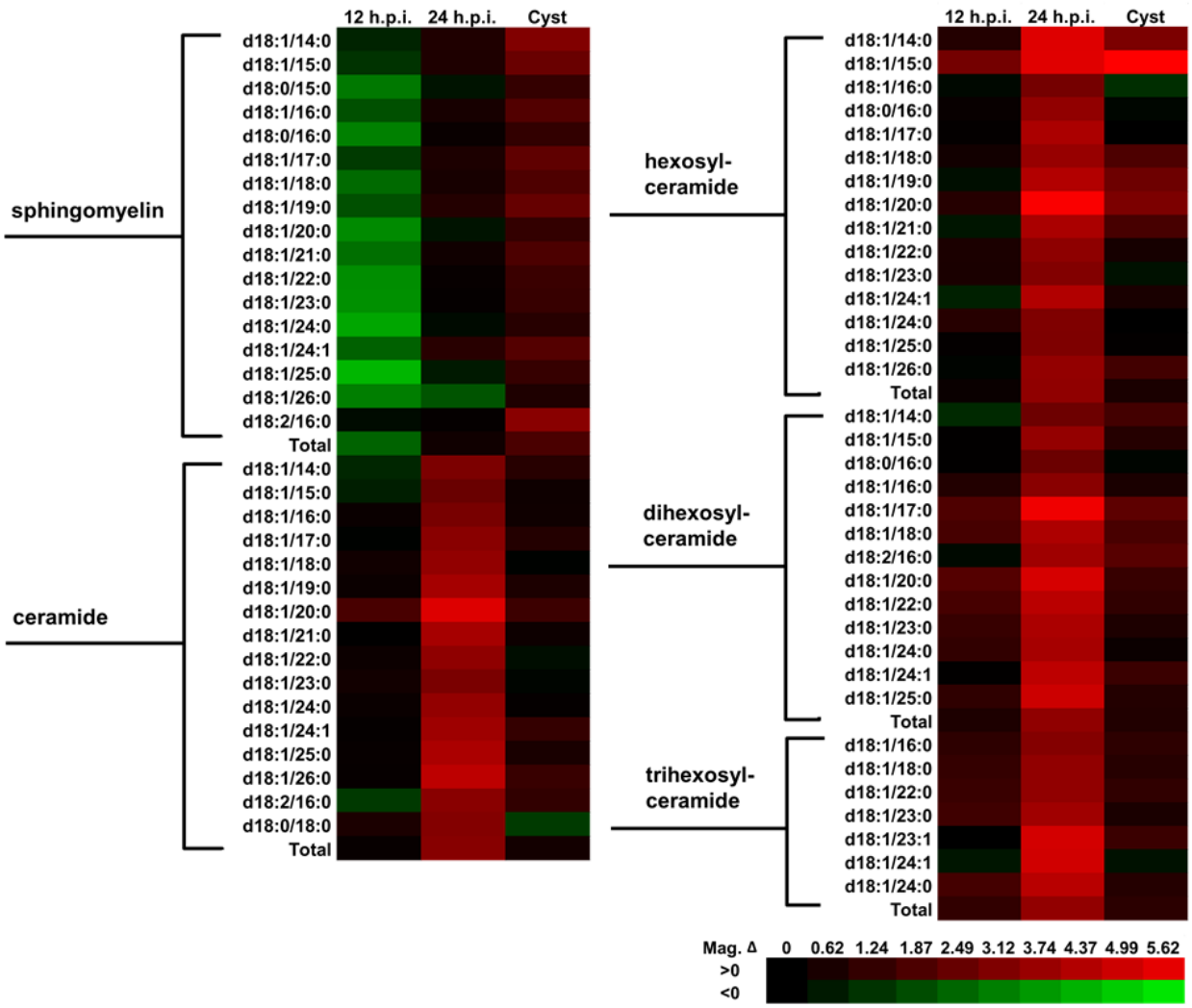

Figure 2.16: Heat map illustrating relative changes in neutral sphingolipid species.

2.2.4 Ceramide-sphingomyelin interplay

Although all neutral SLs increase during encystation, they do not increase to the same extent and therefore the percentage of total SL (Fig. 2.17) described by Cer becomes larger during encystation (~11% in trophozoites to ~44% by 24 h.p.i.). While the percentage described by SM is reduced (~87% in trophozoites to ~46% by 24 h.p.i.) indicating hydrolysis of SM likely as a result of gASMLPD3b1 and/or gASMLPD3b2. During this same period the percentage of trihexosylceramide and dihexosylceramide are doubled (from less than 1% to 3 and 4%

respectively). Between 24 h.p.i and water resistant cysts (~48 hours) there is an increase in SM concentration (Fig. 2.15B), which leads to a compositional shift resulting in SM accounting for ~94% of the total SL in cysts. The differences during encystation can be accounted for at least in part by an increase in Cer concentration and percentage in encysting media vs. culture media (Fig. 2.17B) where 11% of SL in culture media is Cer which increases to 20% in encysting media. However this does not explain the dramatic increase in SM found in the cyst, more so because SM is lower in encysting media than culture media (65% vs. 77%).

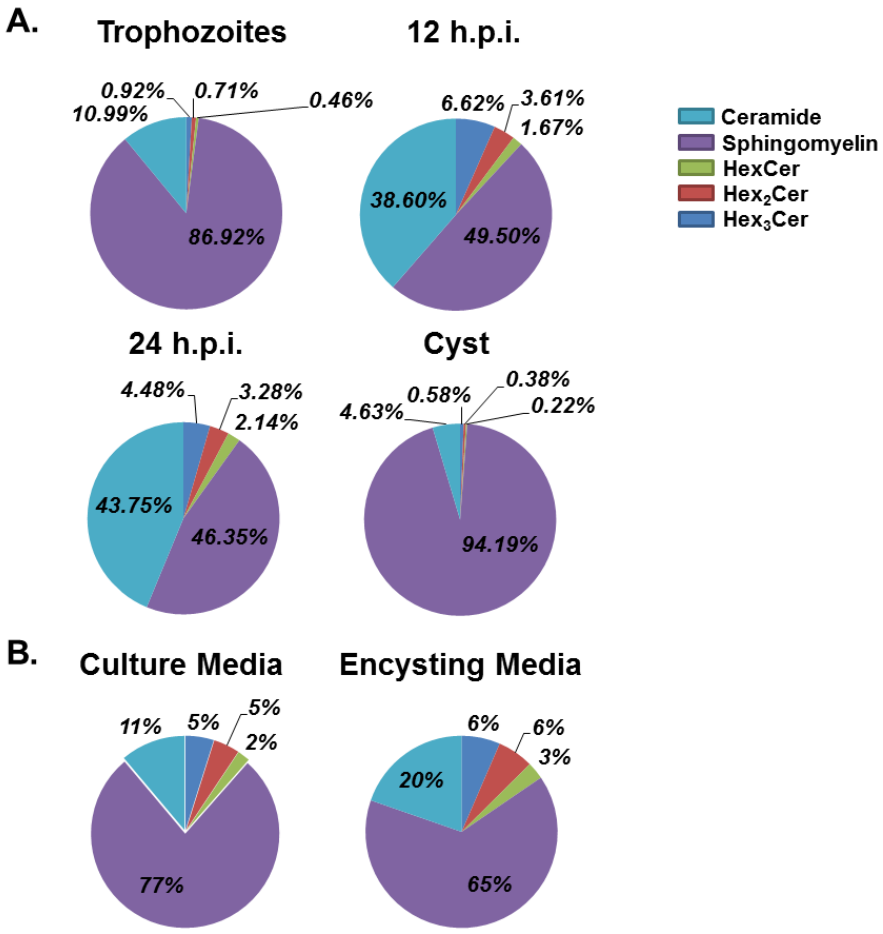

Figure 2.17: Percent composition of sphingolipids by class during differentiation

A. Demonstrates the total SL composition by lipid class in trophozoites, 12 and 24 h.p.i. and water resistant cysts. A shift from high SM to nearly equivalent Cer/SM occurs by 24 h.p.i.

then returns to high SM in cysts. B. shows that this change is not due to differences in the SL composition between culture media and encystations media.

We have been unable to identify any SM synthase gene in the *Giardia* Genome Database (www.giardiaDB.org); however that does not preclude the possibility that they are synthesizing this molecule by some unknown mechanism. Additionally, although the cyst wall is purported to isolate the cells from the environment, it is possible that they are continuing to uptake SM from the culture media during cyst wall formation or even after the wall has been produced completely. Given that transcriptional evidence suggests reduced SMase production in cysts (Hernandez *et al.* 2008; Morf *et al.* 2010), it would not be unreasonable to speculate that this lipid is no longer being hydrolyzed and as a result, stored by the parasite for future use during excystation.

2.3 CONCLUSION

SLs are important bioactive lipid-mediators of eukaryotic cells. These molecules are critical components of the plasma membrane as well as signaling pathways for a diverse range of functions from differentiation to apoptosis. Bioactive SLs such as Cer and SM have been shown to mediate these functions based in part upon the combination of acyl chain and sphingoid base. Here, I report for the first time the sphingolipidome of *Giardia lamblia* throughout its life cycle. It was observed that these lipids are differentially taken up from the extracellular sources and differentially regulated during encystation. There is evidence that longer chain ceramides are favored during cyst formation and the fact that the intracellular and extracellular SL compositions are not identical indicates that *Giardia* remodel these lipids to suit their requirements. In accordance with previous reports for glycosphingolipid changes during encystation (Stefanic *et al.* 2010), I show that trihexosylceramide levels increase dramatically by 24 h.p.i., contrary to these reports however, I found that the same is true for both mono and dihexosylceramides. The interplay between ceramide and SM during cyst formation and

subsequent storage of SM in the cyst form is a novel finding which suggests that the metabolism of SM may be important for the production of cysts. This investigation provides support for a number of future investigations into the mechanism of SL regulation (uptake, remodeling, hydrolysis) as well as the effects that these molecules have on cyst formation and the outcome of cyst formation should this regulation be disrupted.

Chapter 3: Regulation of Sphingomyelin

Sphingomyelin (SM) is the most abundant SL in eukaryotic cells, and *Giardia* is no exception to this. However, as shown above, during cyst formation the log difference between SM and ceramide is reduced such that they are nearly equivalent in abundance. This dramatic change indicates an important role for the modulation of this SL which is likely achieved through the action of giardial SMase enzymes. Furthermore, the subsequent abundance of SM in cysts is a possible indicator of cyst viability and requires further investigation.

SM is a major constituent of membrane microdomains (Bartels *et al.* 2008; Simons and Sampaio 2011; Slotte 2013) or lipid rafts. Lipid rafts are discreet aggregations of lipid rich in SM, cholesterol and PC that have been shown to play important roles in cellular signaling (Lingwood and Simons 2010; Simons and Gerl 2010). Regulation of SM in these rafts is achieved through membrane bound hydrolytic enzyme neutral SMase, which cleaves the head group forming Cer and phosphocholine. In humans there are at least seven SMase enzymes, the activity of which are pH dependent as well as both cell and tissue specific [reviewed in (Liu *et al.* 1997; Goni and Alonso 2002; Zeidan and Hannun 2010)]. Acid SMase is lysosomal and defects in the synthesis of this enzyme in humans leads to the lysosomal storage disorder Niemann Pick disease (Vanier 2013). Neutral SMases are a very large family associated with maintenance of Cer/SM in lipid rafts at the plasma membrane. The alkaline SMases are associated with regulation of SM within the nucleus of cells but are better known as digestive enzymes in the intestine.

As mentioned previously *Giardia* maintain two copies of acid SMase-like phosphodiesterase 3b precursors i.e., gASMLPD3b1 and gASMLPD3b2. In humans, SMPDL-3b is associated with the protective effect of rituximab in preventing focal segmental glomerulosclerosis (FSGS) after kidney transplantation (Fornoni *et al.* 2011). The authors hypothesized that this protective effect is achieved by preventing the down regulation of SMPDL-3b thereby protecting against FSGS by maintaining the integrity of the actin

cytoskeleton and podocyte generation. This hypothesis is supported by the finding of that rituximab treatment of lymphoma cells regulates raft associated ASMase (Bezombes *et al.* 2004). Taken together these reports identify a possible association between SMPDL-3b and raft associated cytoskeletal remodeling, just such remodeling as is required during cyst formation in *Giardia lamblia*.

I investigated SM uptake as well as SMase activity during stage differentiation in *G. lamblia*. I found that both gASMLPD3b1 and gASMLPD3b2 are functional enzymes which are differentially expressed throughout encystation. I also noticed that *Giardia* uptake SM at all stages during differentiation, including cysts and that viable cysts are more abundant in this SL. Modulation of SM is mediated at least in part by gASMLPD3b1 which localizes to discreet areas throughout the cytoplasm of *Giardia* most likely associated with the TVN and overexpression of gASMLPD3b1 reduces excystation efficiency *in vitro*.

3.1 MATERIAL AND METHODS

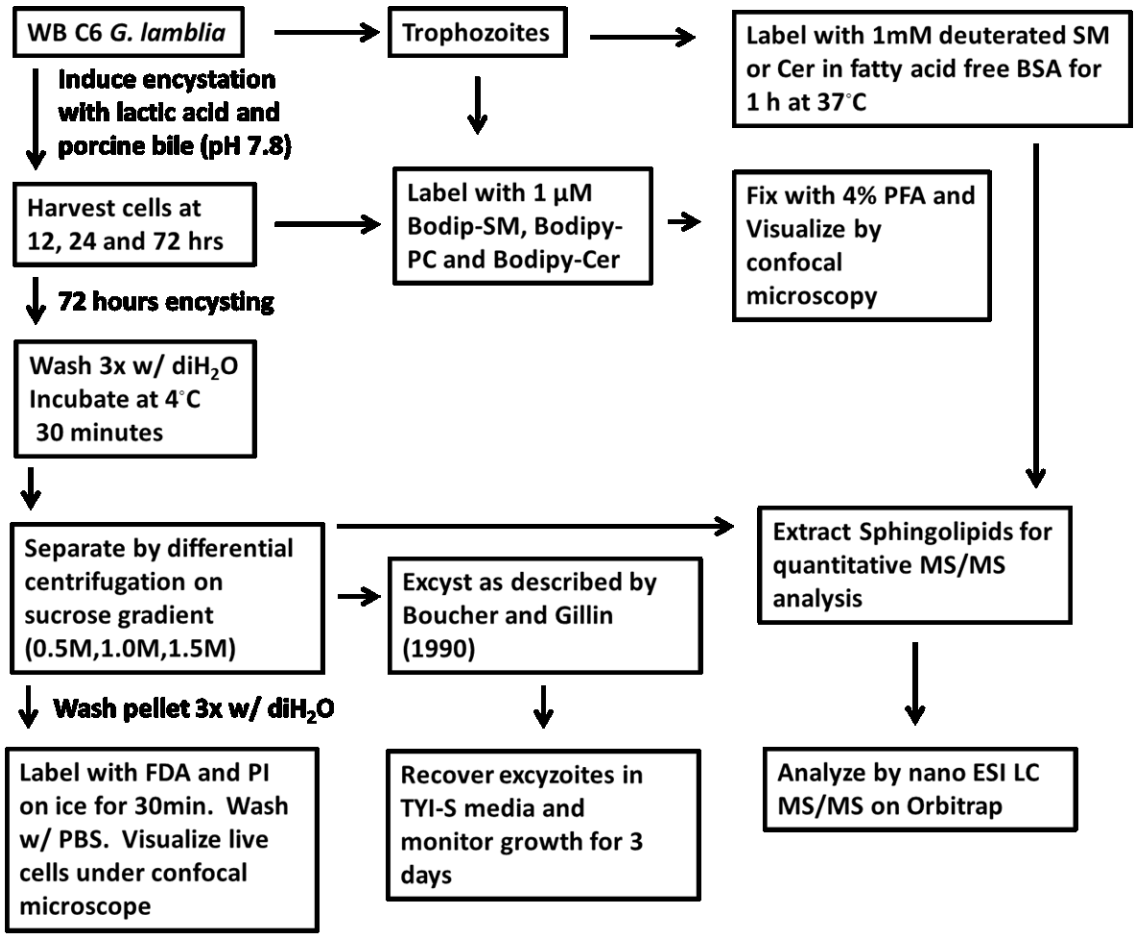

Figure 3.1: Flow chart of methods for chapter 3

3.1.1 Deuterated Sphingomyelin and Ceramide Labeling

Approximately, $1x10^7$ trophozoites were harvested as described above and re-suspended in 1 ml of labeling media (i.e., TYI-S-33 media, pH 7.1 without bovine serum or bile) for 1 h at 37 °C. 100 µl of 100 nmol/µl deuterated sphingomyelin (D_{31} d18:1/16:0) or deuterated ceramide (D_{31} d18:1/16:0) in PBS with 0.1% BSA (fat-free) was added and incubated for an additional hour at 37 °C. Cells were washed in PBS containing 0.1% BSA and centrifuged, and SLs were extracted and analyzed as described above for quantitative sphingolipidomics.

3.1.2 Incorporation of fluorescent tagged lipids

To identify uptake of lipids during cyst formation, trophozoites, encysting cells (24 h.p.i.) and fractionated cysts (1.0M, 1.5M and Pellet) were harvested as described above. Each was

then incubated for 1h in serum and bile free TYI-SS media followed by addition of Bodipy-SM, Bodipy-Cer or Bodipy-PC (1uM final concentration) and incubated for an additional 1h at 37 °C. cells were then washed 3x in PBS, fixed with 4% PFA for 15min at RT and mounted onto microscope slides in DAKO mounting media. Samples were analyzed in a confocal microscope (Carl Zeiss Laser Scanning Systems LSM 700), using the Zen 2009 software (Carl Zeiss) for acquisition and image analysis.

3.1.3 Isolation of cysts by sucrose-density gradient

The step gradient of sucrose (0.5 M, 1.0 M and 1.5 M) was formed in round-bottom glass tubes (13 x 100 mm). Water-resistant cysts harvested as described above were re-suspended in 1 ml sterile water applied on the layer of the gradient and centrifuged for at 400 × g for 30 min at 4 °C. The cysts formed distinct clusters at the 0.5 M and 1.0 M interface (1.0 M), the 1.0 M and 1.5 M interface (1.5M), and also at the bottom of the tube (Pellet). Cysts were collected from each layer by carefully pipetting and then washed extensively in cold, distilled H_2O prior to processing for subsequent analyses as described in the text.

3.1.4 Cyst viability

Fluorescein diacetate (FDA) inclusion and propidium iodide (PI) exclusion experiments were performed to monitor cyst viability. Briefly, a 25 mm stock solution of FDA and PI (Sigma) was prepared in 100 mm phosphate buffer, pH 6.0, from which a working solution was made by adding 40 µl of stock to 10 ml of phosphate buffer. Cyst fractions were collected as described above. Approximately 10^7 cysts were subjected to FDA and PI staining as described previously by Gillin colleagues (Mendez *et al.* 2013). Cysts were washed in PBS, re-suspended in DAKO mounting media, and mounted on a glass microscope slide. Samples were analyzed on a confocal microscope (Carl Zeiss Laser Scanning Systems LSM 700), using the Zen 2009 software (Carl Zeiss) for acquisition and image analysis.

3.1.5 Recombinant gASMLPD3b1 and gASMLPD3b2

Plasmid Construction

The entire open reading frames of gASMLPD3b1 and gASMLPD3b2, ORF_8360 and ORF_16737 respectively, were amplified by PCR using the primers 5'-ATGCGAATCCATGTTCTTGGCCGTGCTGCTCCTCTCT – 3'and 5' – GCATTGCGGCCG CCTGCAACTTGGCTAAACATGACTTGTATGACTC – 3' for gASMLPD3b1 and 5' – ATGCG AATCCATGAAGGCCCTCTTTTACATAGGTTTG – 3' and 5' – GCATTGCGGCCGCGTTG GAGTTGCTAAGGTTATACGCGTC – 3' for gASMLPD3b2. The purified PCR products were digested with EcoR1/Not1 and independently ligated into EcoR1/Not1 digested pT7CFE1-CHIS expression vector (Thermo Scientific). The new plasmids pT7CFE8360cHIS and pT7CFE16737cHIS were then transformed into competent DH5α cells and plated onto LB plates containing 100μg/ml ampicillin. Colonies were screened by PCR and positive colonies were sequenced at the University of Texas-El Paso (UTEP) DNA core facility. The ABI Prism BigDye Terminator v3.1 Cycling Sequencing Kit (Applied Biosystems, Carlsbad, CA) was used to amplify the DNA with fluorescently labeled dideoxynucleotides. The sequencing reaction was subsequently cleaned using Agencourt Clean SEQ (Beckman Coulter, Brea, CA).

In-vitro translation

Plasmids were purified with Qiagen midi-prep kit excluding addition of RNaseA to resuspension buffer (Qiagen). DNA was diluted to 0.5μg/μl and used as template for *in vitro* translation using the 1-Step Human High-Yield Mini IVT Kit (Thermo Scientific) according to manufacturer's instructions. A positive control expressing green fluorescent protein (GFP) and a template free negative control were included. Translation efficiency was assessed by western blot analyses using anti-HIS antibody (Promega). Translated protein was used immediately or stored at -20 °C for no more than one week.

3.1.6 Sphingomyelinase Activity

Sphingomyelinase (SMase) activity was assayed with the Amplex Red Sphingomyelinase assay kit according to manufacturer's instructions (Invitrogen) using the one-step method to assay neutral sphingomyelinase activity and the two step method to assay acid sphingomyelinase activity. For each assay, fluorescence measurements were normalized to protein concentration.

3.1.7 Cleavage of NBD-SM

For initial validation of SMase activity of *in vitro* translated (IVT) protein, SM hydrolysis was monitored as described previously (Loidl *et al.* 2002). Briefly, equivalent concentrations of protein from gASMLPD3b1 and gASMLPD3b2 as well as negative control IVT reactions were incubated in neutral (200mM Tris, pH7.4 10mM MgCl), Acid (50mM NaOAc, pH 5.0) or Acid with Zinc (50mM NaOAc, pH 5.0 10mM ZnCl) buffer with 1uM (final concentration) NBD-SM for 2 h at 37 C. The reactions were stopped by addition of 600 µl $CHCl_3$:MeOH 2:1, vortexed briefly, then centrifuged at 5000 xg for 5min. The lower $CHCl_3$ phase was transferred to a fresh tube, dried under N_2 and resuspended in 10uL $CHCl_3$:MeOH 1:1. 5uL of each reaction was loaded onto HPTLC plates with 5uL Microcaps™ (Drummond Scientific). HPTLC was resolved in 65:25:4 $CHCL_3$: MeOH: H_2O.

3.1.8 Overexpression of gASMLPD3b1 in *Giardia*

Plasmid Construction

For overexpression, a small peptide-epitope (AU1)-tagged pNT5 expression plasmid (obtained from Dr. Chin-Hung Sun, Taiwan) containing gASMLPD3b1 gene under control of the constitutive alpha2 tubulin promoter was constructed following the method described by Pan et al. (Pan *et al.* 2009). The entire open-reading frame of gASMLPD3b1 ORF_8360 was amplified by PCR using the primers 5'-GCGCCATGGGGATG TTCTTGGCCGTGCTGCTC-3' and 5'-GCGGAATTCTCAGATGTATCGATACGTATCCTG CAACTTGGCTAAACATG -3'. The insert was digested with EcoR1/Nco1 and ligated into EcoR1/Nco1-digested dephosphorylated pNT5 plasmid (Pan *et al.* 2009). This new plasmid pN8360cAU1 was then transformed into

competent DH5α cells and plated onto LB plates containing 100μg/ml ampicillin. Colonies were screened by PCR and positive colonies were sequenced at the University of Texas-El Paso (UTEP) DNA core facility. The ABI Prism BigDye Terminator v3.1 Cycling Sequencing Kit (Applied Biosystems, Carlsbad, CA) was used to amplify the DNA with fluorescently labeled dideoxynucleotides. The sequencing reaction was subsequently cleaned using Agencourt Clean SEQ (Beckman Coulter, Brea, CA).

Transfection

The parasites were placed in a 4-mm electroporation tube (Fisher Biotech, Waltham, MA) in a 300-μl suspension of TYI-SS media where 40μg of the pN8360cAU1 plasmid was added. Trophozoites were then transfected by electroporation on a BioRad Gene Pulser X cell (BioRad, Hercules, CA) using the following parameters: 322 V, 500 μF, and ∞Ω resistance (4-mm cuvette). Cells were allowed to recuperate in media overnight, followed by selection with 150μg/ml G418 (Sigma Aldrich, St. Louis, MO). Stable transfectant trophozoites overexpressing gASMLPD3b1 (+SMPDL-3b1) were established within two weeks.

3.1.9 Western blot analysis

Parasites were harvested and resuspended in lysis buffer (5mM Tris HCl; Triton X-100; 0.1%; pH 7.4) containing protease inhibitor cocktail and E-64 (1 μM, Sigma). The sample was freeze thawed at -80 °C followed by sonication. This crude lysate, or IVT protein, was boiled in sample buffer before being analyzed (100 μg protein/lane and 10μg protein/lane respectively) by 10% SDS-PAGE, and was followed by immunoblotting analysis on the polyvinylidene fluoride (PVDF) membrane. The membrane was blocked in 1% BSA, incubated with appropriate primary antibody, anti-AU1 antibody (1:200 monoclonal, Covance) or anti-HIS antibody (1:200 monoclonal, Promega) and incubated overnight at 4 °C. The PVDF membrane was then incubated with anti-mouse HRP conjugate (1:10,000; KPL, Inc., Washington, DC) for 1h at room temperature. The enhanced chemi-luminescence (ECL) technique was used for the detection of protein bands.

3.1.10 Staining with anti-AU1 antibody for immunofluorescence

To monitor the cellular localization of SMPDL-3b1, cells (+SMPDL-3b1) were labeled with mouse ascites anti-AU1 antibody (1:200, Covance). Cells were harvested and fixed to slide covers using 4% paraformaldehyde (PFA) followed by permeabilization with 0.2% Triton-X100. Fixed samples were allowed to react with anti-AU1 antibody overnight at 4 °C, followed by reacting with anti-mouse Alexa Fluor® 568 (Invitrogen). Cells were subsequently incubated with 4', 6-diamidino-2-phenylindole (DAPI; Invitrogen) and mounted with DAKO mounting media (Agilent Technologies). Samples were analyzed in a confocal microscope (Carl Zeiss Laser Scanning Systems LSM 700), using the Zen 2009 software (Carl Zeiss) for acquisition and image analysis.

3.1.11 Staining of Lysosome and Endoplasmic Reticulum

To determine likely cellular localization of ASMLPD-3b1 cells were labelled with ER-tracker™ Green or LysoTracker® Green DND-26 (Invitrogen) according to manufacturer's instructions and compared staining with anti-AU1 antibody by confocal microscopy. Cells were allowed to attach to microscope slide covers in TYI-SS media at 37 °C for 15 minutes. The media was then aspirated and replaced with Hepes buffer (pH7.1) containing 100nM ER-tracker™ green or LysoTracker® Green DND 26. These were incubated for an additional 15 minutes at 37 °C, then inverted onto microscope slides and visualized within 10 minutes in a confocal microscope (Carl Zeiss Laser Scanning Systems LSM 700), using the Zen 2009 software (Carl Zeiss) for acquisition and image analysis.

3.1.12 Detection of secreted protein in spent media

To determine if gASMLPD3b1 is secreted from the cell, western blot was performed with proteins extracted from the spent media. 25cm2 flasks were of +gASMLPD3b1 trophozoites were grown to early log phase. 50ml of spent culture media was decanted and centrifuged at 20,000 x g for 30min, transferred to fresh tube and centrifuged at 20,000 x g for an additional 15 min. Cleared media was then dialyzed extensively against 5mM Ammonium Bicarbonate for 24

h at 4°C followed, frozen and lyophilized. Lyophilized samples were resuspended in 5ml lysis buffer (100mM Tris-HCL 0.2% triton x-100 pH 7.4), protein was quantified by Bradford assay (BioRad) and 100µg of protein was used for SDS-PAGE followed by Western Blot as described above.

3.2 RESULTS

3.2.1 Cysts rich in SM are viable and excyst efficiently

The production and maintenance of viable cysts by *Giardia* is critical for establishing infection (giardiasis) in its mammalian host. Earlier reports suggest that gGlcT1 by this parasite is linked to cyst viability (Mendez *et al.* 2013). It was also reported by Gillin et al. (1989) that giardial cysts produced in culture (i.e., *in vitro*-derived) are of two kinds—oval-shaped classical cysts with refractive cyst walls (type I) and non-classical/non-oval-shaped (type II) cysts. It is interesting to note that *in vitro*-derived cysts are generally less viable than natural cysts and only type-I cysts are viable and undergo excystation both *in vivo* and *in vitro* (Boucher and Gillin 1990). Because our results show that SM concentrations are high in cysts (Fig 2.15 and 2.17), we asked if the increased levels of SM could be an indicator/determinant of cyst viability. In order to investigate this, *in vitro*-derived cysts were subjected to sucrose-density gradient centrifugation as described in Materials and Methods. Gradient centrifugation yielded three populations of cysts based on their buoyant densities i.e. cysts found in 1.0 M and 1.5 M gradients as well as sediment (as a pellet) at the bottom of the tube (Fig. 3.2). To assess viability, these three populations of cysts were labeled with cell-permeable fluorescein diacetate (FDA) and the cell-impermeable nucleic acid staining agent, propidium iodide (PI) (Mendez *et al.* 2013). Although the morphology of cysts in the pellet fraction was consistent with what would be expected from viable cysts (ovoid, thick cyst walls), we found that the majority (~98%) of cysts in this fraction are non-viable (Fig. 3.2 A v,vi; B i). While cysts from 1.5 M fraction show ~15% viability, 1.0 M cysts contain the highest percentage of viable (~40%) cysts.

Because FDA/PI assay is an indirect measure of viability (Smith and Smith 1989), we carried out *in vitro* excystation experiments following the protocol described by Gillin and Boucher (Boucher and Gillin 1990). However, given that the assessing of excyzoites by microscopy can be erroneous, we placed excysted cells in fresh culture media and monitored the growth of trophozoites for 72 h. It was observed that the cysts collected from 1.0 M fraction showed maximum excystation, with nearly every tube containing sufficient excyzoites to show growth within the allotted time (Fig. 3.2 B ii).

To identify a possible correlation between viability and SL abundance, we performed quantitative MS analyses. Analyses revealed that although Cer and GSL concentrations within cysts are higher than trophozoites, the 1.0 M fraction consistently has the highest level of SLs compared with the other two cyst fractions. Furthermore, the SM level is highest within the 1.0 M fraction (significantly higher than the 1.5 M fraction and trending higher than the pelleted fraction) indicating a possible link between cyst viability and SM concentration (Fig. 3.2 C).

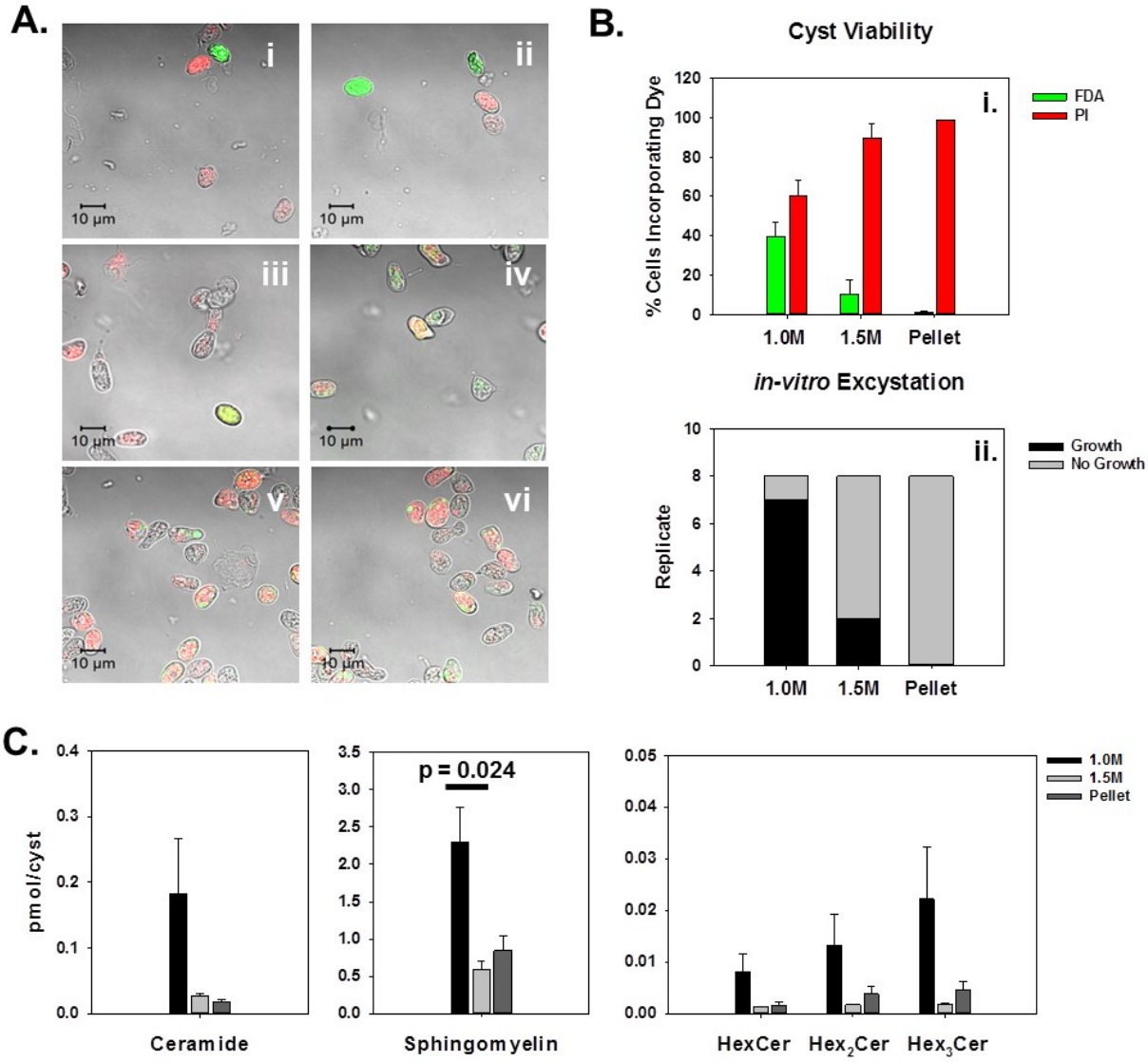

Figure 3.2: Viability of cysts separated by density centrifugation.

A. Representative confocal images showing labeling of FDA (green) and PI (red) in 1.0M fraction (i, ii) 1.5M fraction (iii, iv) and pellet (v,vi). B. i. Quantitation of microscopy, graph represents the percentage of cells out of 100 for each sample incorporating either FDA (viable), PI (non-viable) or both (non-viable). ii. *in vitro* excystation of cysts from each fraction. The graph shows the result of three separate excystation experiments followed by culture for 72 h; growth was assessed by visual inspection of culture tubes. C. Abundance of SLs in cysts recovered from each of three sucrose fractions

3.2.2 SM is taken up by trophozoites, encysting cells and cysts.

To verify that *Giardia* is able to scavenge SM from the media and hydrolyze to form Cer, we cultured ~1 x 10^7 cells in the presence of deuterated SM followed by the extraction of SL and identified by high-resolution mass spectrometry. SIM of the deuterated SM at 734.7694 identified a very intense peak (10^7), and hydrolyses of that species to ceramide was verified by SIM of deuterated ceramide at 569.7140, which resulted in a peak of less intensity (10^5) that did not appear in control cells. To investigate if SM is synthesized directly from ceramide taken up by the parasite from the media, we cultured ~1 x 10^7 trophozoites in the presence of deuterated ceramide and as expected we identified an intense peak (1.4 x 10^7) at 569.7140. We were unable to identify a peak corresponding to deuterated SM at 734.7694, which suggests that SM that is present in cysts is not synthesized from the ceramide directly. Thus, the large increase in SM in cysts could be due to the continued influx of SM into the cells during encystation without a subsequent efflux of this material or hydrolysis to ceramide.

Because SM is more abundant in cysts than trophozoites, I investigated the incorporation of fluorescent tagged SM in encysting cells as well as cysts. As figure 3.3 shows fluorescent SM, PC and Cer are readily taken up by trophozoites, encysting cells and cysts. However, whereas SM and Cer intensely label cysts, PC is much less intense indicating that this lipid is not incorporated as efficiently into cysts as either Cer or SM. This finding is interesting as it parallels a previous report that the uptake of fluorescent Cer and SM is sensitive to cytoskeleton destabilizing inhibitors, whereas the uptake of PC is not. This suggests that cysts maintain active mechanisms for the transport of SLs into the cell, whereas cytoskeleton independent endocytosis is dramatically reduced.

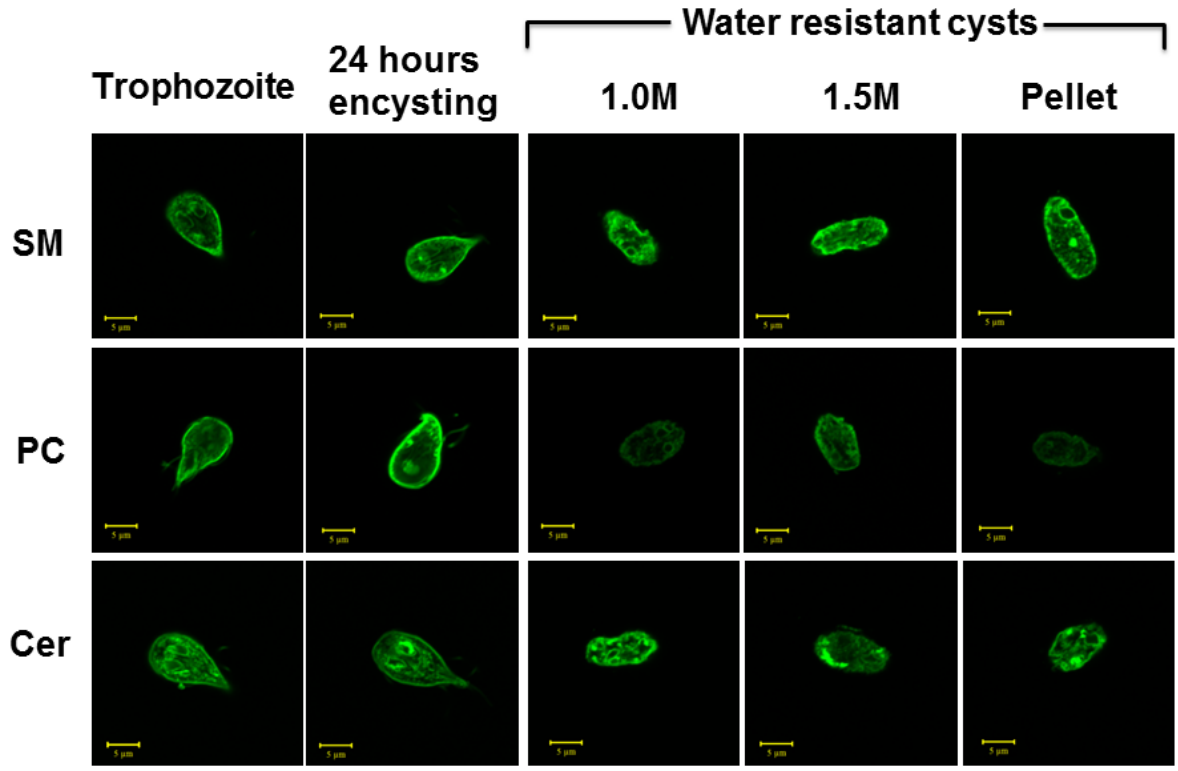

Figure 3.3: Uptake of fluorescent lipids in trophozoites, encysting cells and cysts.

3.2.3 ASMLPD3b1 and ASMLPD3b2 are both active enzymes

The genome sequence of *Giardia* predicts two SMase genes, gASMLPD3b1 and gASMLPD3b2. Previously, we have reported that transcription of these enzymes changes during differentiation, with increased transcription at 6 and 12 h.p.i. (Hernandez *et al.* 2008). Proteomics studies have identified peptides aligning with ASMLPD-3b1 but not ASMLPD-3b2 (Jedelsky *et al.* 2011). Analysis of these proteins with the Sanger institutes database of protein families Pfam (Punta *et al.* 2012), indicate that gASMLPD3b2 contains a calcineurin-like phosphoesterase domain as well as pfamB-682 domain whereas due to 2 point mutations in the metal binding domain Pfam does not recognize the phosphoesterase domain of gASMLPD3b1. Similar to both gASMLPD3b2 and human SMPDL-3b, gASMLPD3b1 does contain the pfamB-682 domain, however the function of this domain is unclear. Taken together these data are inconclusive, though both enzymes are transcribed only one was found to be translated by

proteomics screens, however that enzyme does not possess a clear functional phosphodiesterase domain.

To resolve these questions and confirm that the two *Giardia* SMase enzymes are indeed able to catalyze the hydrolysis of sphingomyelin to ceramide, I performed in-vitro translation of recombinant gASMLPD3b1 and gASMLPD3b2 with C-terminal His-tags followed by fluorescence assays under both acidic and neutral conditions.

Both enzymes were readily translated and identified by western blot (Fig. 3.4A), however as is often the case with lipid metabolic genes, even under these conditions both are insoluble in the reaction mixture, therefore purification was not possible. Insolubility was not due to misfolding because I found that both enzymes are able to hydrolyze SM to Cer (Fig. 3.4C). Quantitation of this hydrolysis using the Amplex Red (Invitrogen) indirect SMase assay suggests that, whereas gASMLPD3b2 shows similar activity in both acidic and neutral buffers, gASMLPD3b1 activity is significantly inhibited in neutral buffer (pH 7.4) yet displays high activity in acid buffer (pH 5.0). This is unexpected considering the PIs of these enzymes are 5.7 and 6.5 respectively. Of course it is possible that the decrease in activity of gASMLPD3b1 is due to the effect of magnesium in the neutral assay buffer as exemplified by the strong inhibition of activity in acid buffer after addition of zinc. Further experiments should be performed to investigate the effects of other divalent cations in this assay system. Given high activity of gASMLPD3b1 in acidic conditions, it is likely that this enzyme is not involved in the hydrolysis of SM at the plasma membrane, and is likely confined either to lysosomal like compartments (PVs or the TVN) or is secreted from the cell. These are both supported by a recent report identifying gASMLPD3b1 as an *N*-glycosylated protein likely secreted or membrane bound within lysosomes (Ratner *et al.* 2008). Although the predicted molecular weight of gASMLPD3b1 is ~50kD, the enzyme consistently migrates at ~45kD on SDS-PAGE. This indicates possible cleavage of the enzyme at the amino terminus and likely removal of the transmembrane domain (~20 amino acids, 4kD) providing evidence that this enzyme could be secreted to the cell exterior. The promiscuous activity of gASMLPD3b2 is also interesting and

suggests that in vivo this enzyme could be membrane bound at the plasma membrane. Further investigation into this is required to identify the cellular context of these sphingomyelinase enzymes.

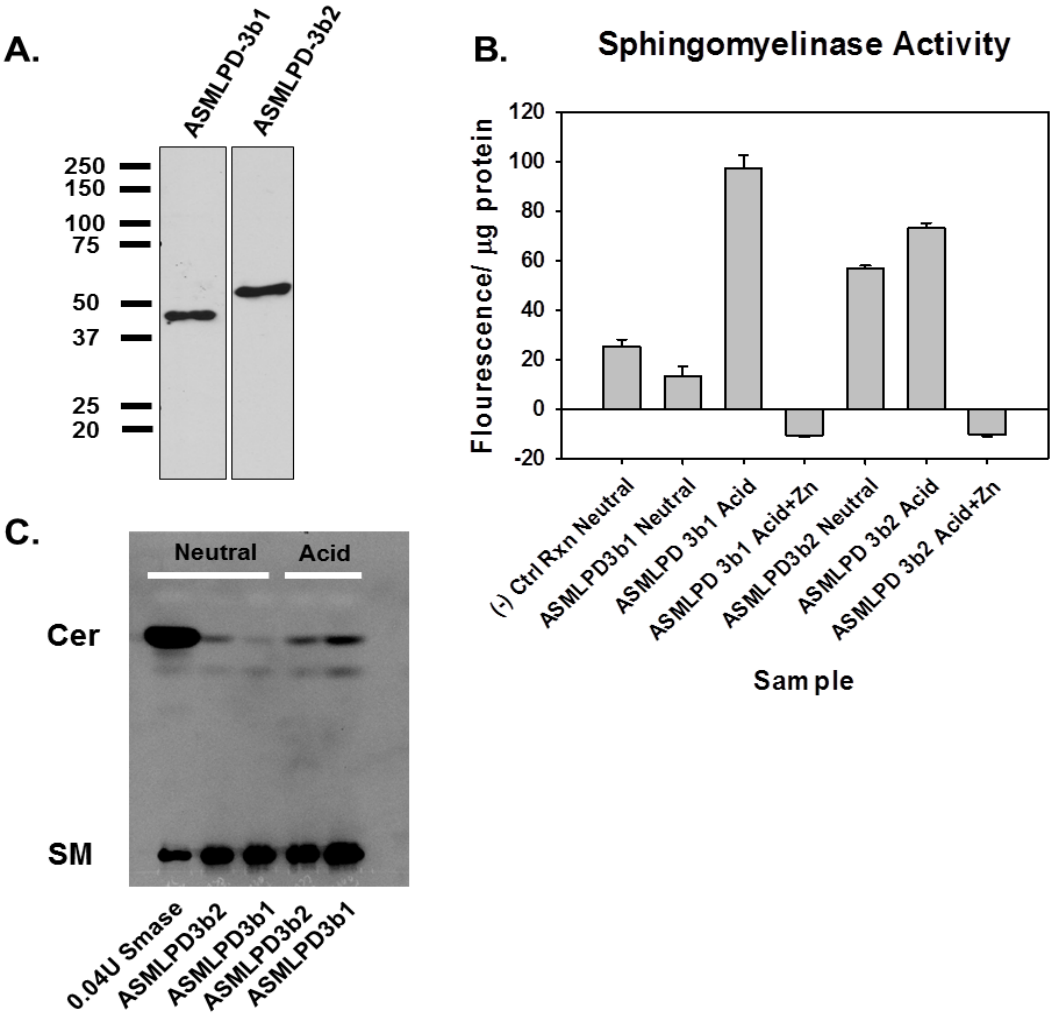

Figure 3.4: Expression and activity of recombinant sphingomyelinase

A. Western blot probed with anti-His antibody showing translation of recombinant enzymes. B. Sphingomyelinase activity under various conditions. Activity presented as fluorescence (excitation 530/ emission 560) per µg of protein in each reaction. C. HPTLC of

NBD SM hydrolyzed by control Sphingomyelinase (from *B. cereus*), gSMDL-3b1 and gASMLPD3b2 under neutral and acidic conditions.

3.2.4 gASMLPD3b1 localizes to the TVN but not PVs

As stated earlier the ultrastructure of *Giardia* cells is quite different from higher eukaryotes. The parasite lacks mitochondria, peroxisomes and lysosomes. The primitive Golgi is found as a transient structure present only during encystation. In the place of some of these organelles the parasite has organelles whose function has not been established (mitosome) or whose function is altered (acidified peripheral vacuoles). The ER of *Giardia* is part of a labyrinthine TVN proposed to act as both ER and an endosomal/lysosomal compartment (Abodeely *et al.* 2009). Acidified peripheral vacuoles traditionally believed to be lysosomes may be the sites of clatherin mediated endocytosis (Hernandez *et al.* 2008; Abodeely *et al.* 2009) and either fuse to or are contiguous with this TVN.

Because of the acidic pH optimum for gASMLPD3b1, I hypothesized that this enzyme would inhabit these acidified vesicles which reside just under the plasma membrane and serve to break down SM as it was taken up from the extracellular milieu. However, immunofluorescence with anti-AU1 antibody coupled with both lysosome and ER labeling dyes suggests that this is not at all the case. In fact, although under the current experimental conditions it is not clear if gASMLPD3b1 is localized to the TVN or another discreet vesicle, it is clear that it does target to the perinuclear membrane as well as a tubular network similar to the TVN (Fig 3.5C arrows) and it does not localize to the PVs (Fig 3.5C arrow heads). Of course LysoTracker® is designed to label acidified compartments and it would appear that these also form a complex network within these cells. I hypothesize that this is because the TVN and PV are in fact contiguous, therefore in areas where these organelles intersect the pH is low enough to label with LysoTracker as well as provide an environment suitable for SMase activity. It is possible that, precisely because of

gASMLPD3b1 residence within this network, the enzyme is so dramatically inefficient at higher pH, indicating a possible mechanism for controlling unwanted SM hydrolysis in the ER.

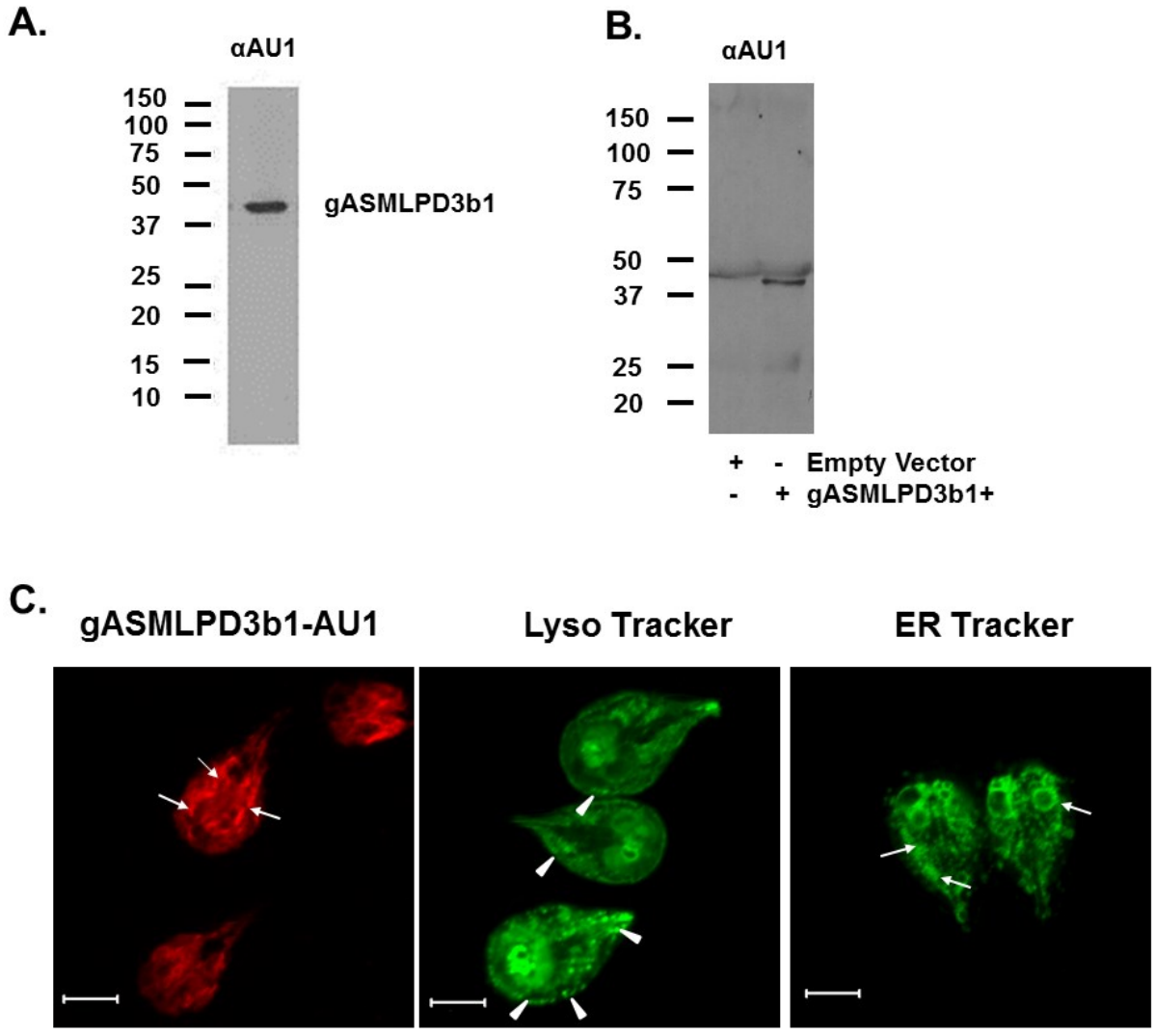

Figure 3.5: Cellular localization of gASMLPD3b1, ER and acidified vesicles in *Giardia*

A. Western blot probed with anti-AU1 antibody showing specificity for gASMLPD3b1-AU1 B. Identification of gASMLPD3b1-AU1 in spent media C. gASMLPD3b1 localizes to a

tubular structure as well as the perinuclear membrane similar to the ER marker (arrows). However it does not localize with the acidified peripheral vacuoles (arrow heads). Bar = 5μm

3.2.5 gASMLPD3b1 is secreted from the cell*

Because gASMLPD3b1 is an N-glycosylated protein and potentially secreted from the cell, I analyzed spent culture media for the enzyme. Western blots probed with anti-AU1 antibody did reveal the presence of the recombinant enzyme in these samples (Fig. 3.5 B). This is a novel finding and requires further investigation. Previous reports have identified that Giardial cells co-cultured with human epithelial cells (caco-2) results in membrane dysfunction of these cells associated with both secretion of unknown *Giardia* factors as well as adhesion by the parasite (Ringqvist *et al.* 2008; Maia-Brigagao *et al.* 2012). Interestingly, exogenous addition of sphingomyelinase to this same cell line leads to a similar disturbances in cell barrier function (Bock *et al.* 2007). Further experiments should pursue this possible link between Giardia virulence and possible sphingomyelinase disruption of host epithelial barrier function.

3.2.6 gASMLPD3b1 overexpression reduces excystation efficiency

Sphingomyelinase is a key regulator of the composition of plasma membranes and therefore increased activity of these enzymes could lead to a destabilization of lipid rafts. Furthermore, the product of sphingomyelinase, Cer, is a potent activator of a wide range of cellular signaling pathways linked to autophagy, senescence, differentiation and apoptosis (Obeid and Hannun 1995; Liu *et al.* 1997; Hannun and Obeid 2008). My mass spectrometry analyses indicated that SM is abundant in viable cysts and therefore represents a possible target for prevention of excystation, a critical event in the life cycle of Giardia for maintaining infectivity.

I asked if the effect of increased SM hydrolysis caused by overexpression of gASMLPD3b1-AU1 would interfere with growth, encystation or excystation of *Giardia*. Initial experiments suggest that cells overexpressing this enzyme grow at the same rate as empty vector transfected controls (Fig 3.6 A) and encystation does not appear to be hindered (not shown).

Interestingly *in vitro* excystation was reduced in cells overexpressing gASMLPD3b1, however this difference was not significant. Excystation efficiency was monitored by counting trophozoites seven days after *in vitro* excystation as described by Gillen and Boucher (1990). It is possible that this lag time (between excystation and quantitation) could be resulting in arbitrarily inflated cell counts for sphingomyelinase overexpressing cells. Alternatively, I have shown that this enzyme is not located at the plasma membrane rather it is located to organelles within the cell and due to it this isolation may play a limited role in the maintenance of SM in cysts. Additional work to overexpress gASMLPD3b2 will potentially shed light on these findings and I hypothesize that this enzyme will be localized to the plasma membrane and exhibit stronger control over SM in cysts.

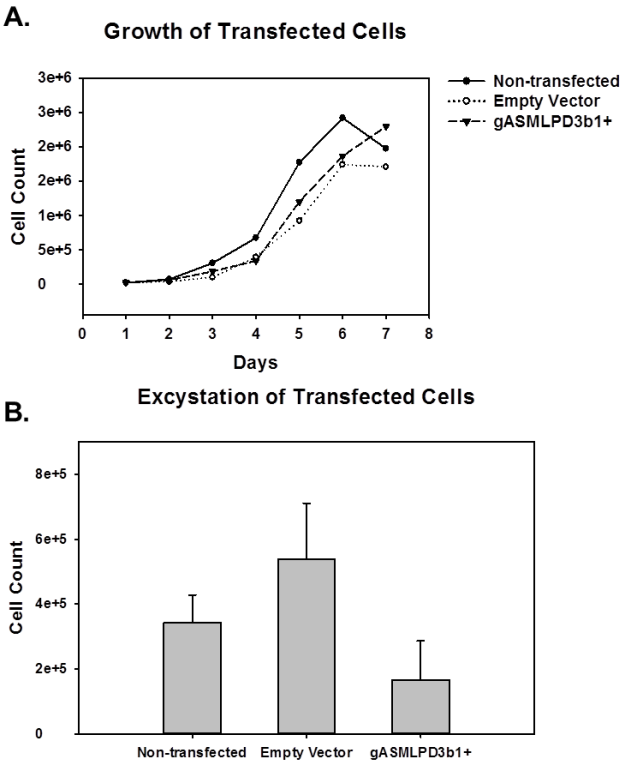

Figure 3.6: Effects of gASMLPD3b1 overexpression on cell growth and excystation

A. gASMLPD3b1 overexpression does not alter vegetative growth of Giardia trophozoites. B Excystation efficiency is reduced in cysts overexpressing gASMLPD3b1.

3.3 CONCLUSION

The transformation from trophozoite to cyst and cyst to trophozoite constitutes the life cycle of *Giardia* and is critical for infecting it mammalian host. I found that the efficiency of excystation correlates with SM content of the *Giardia* cyst, i.e. those cysts that are highest in SM content are more viable and excyst efficiently compared to low SM containing cysts (Fig. 3.1). This is a novel finding, and future studies should be conducted to confirm this and possibly identify the mechanism by which SM could maintain the cyst viability. During excystation cysts pass through acidic pH of the stomach, release two trophozoites, and ultimately colonize in the small intestine (pH ~7.8), where newly emerged trophozoites are exposed to high levels of digestive enzymes, dietary lipids and bile salts

The modulation of SM is carried out by one or both of the *Giardia* SMase enzymes which are differentially expressed during encystation and excystation. I found that both of these enzymes are able to efficiently hydrolyze SM to Cer, furthermore, gASMLPD3b1 localizes to the TVN which houses both lysosomal and ER functions in this parasite. I hypothesize that gASMLPD3b1 is secreted from the cell and may potentially be involved in dysregulation of host epithelial barrier function. Overexpression of this enzyme reduces excystation efficiency supporting the role of SM in maintaining cyst viability. However, given the cellular isolation of gASMLPD3b1 from endocytosed SM, this reduction was not enough to prevent excystation altogether. Future studies will include the overexpression of gASMLPD3b2 followed by examining its role in modulating and maintaining the level of SM in the plasma membrane beneath the cyst wall, which could provide a new mechanism of excystation.

Chapter 4 Discussion

G. lamblia is an evolutionarily conserved organism that likely diverged from higher eukaryotes prior to the mitochondrial fusion event (Hilario and Gogarten 1998). As a result of this conservation or as a result of parasitism (Stechmann and Cavalier-Smith 2002), *Giardia* are highly streamlined in a number of biological processes including glucose metabolism, maintenance of genetic material, protein synthesis and lipid neogenesis (Morrison *et al.* 2007). Absent a great deal of the complexity found in more derived eukaryotes, they represent an ideal model for the study of these pathways. Not only is *Giardia* an excellent model for the academic study of basic biological processes, it is the leading cause of non-bacteria associated diarrhea worldwide. Although only sixty percent of cases are symptomatic, this can be a devastating disease whose acute symptoms of diarrhea and malabsorption can lead to chronic symptoms ranging from failure to thrive, stunting, chronic fatigue, cognitive disorders, and irritable bowel syndrome (Ankarklev *et al.* 2010; Halliez and Buret 2013). The absence of many biological processes found in higher eukaryotes presents a unique opportunity to devise strategies to fight this disease, as those processes which are retained by the organism are likely to be essential for the maintenance of its lifecycle. Previously it was shown that *Giardia* require SLs for growth and encystation. In my dissertation I have elucidated the sphingolipidome of Giardia for the first time. In accordance with the nature of *Giardia* metabolism, this sphingolipidome is simple (as compared with higher eukaryotes) and represents the minimum requirements for SL metabolism during growth as well as differentiation of the eukaryote cell. Parasitism has alleviated the need for *de novo* synthesis of many of these lipid molecules, yet the organism has retained machinery for the manipulation of these molecules indicating that they are essential and modulated actively during encystation.

I have analyzed this modulation to identify specific SL changes during cyst formation. The *Giardia* genome maintains SL metabolism, mediated by the five SL genes i.e. gSPT1, gSPT2, gASMLPD3b1, gASMLPD3b2 and gGlcT1 and the transcription of these genes is

differentially regulated during encystation (Hernandez et al 2008). Previous studies from this and other laboratories have shown that gGlcT1 activity is essential for encystation by *Giardia* (Hernandez *et al.* 2008; Sonda *et al.* 2008; Stefanic *et al.* 2010; Mendez *et al.* 2013). Additionally, the inhibition of SPT by L-cycloserine, interrupted ceramide uptake and targeting in trophozoite cells (Hernandez *et al.* 2008). Given these data, I investigated the changes in SLs during encystation by analyzing the metabolites themselves, rather than the enzymes responsible for their metabolism. I chose this approach in order to cast a broader net that would allow me to identify processes not predicted by the *Giardia* genome as well as to decipher the alterations in SLs that could be correlated directly with changes to enzyme production. To initiate this study, I first standardized a method for the extraction and enrichment of SL species from *Giardia* trophozoites, encysting cells and cysts. I found that the complex nature of *Giardia* cell extracts, coupled with the low abundance of many SL species required extensive separation of these extracts prior to analyses. I analyzed SLs by direct infusion into an ion trap mass spectrometer (LTQ, Thermo) and identified species by total ion mapping and fragmentation analyses. I found that *Giardia* have both neutral and acidic glycosphingolipids, including the neutral mono-, di-, and tri-hexosylceramides as well as hexosamine containing tri-and tetra-hexosylceramides; and the acidic GM1, GM3 and GD3. I also found both Cer and SM, with SM being the most abundant SL. Analyses of culture media sources of SL (bovine serum and bovine bile) showed a very similar profile and I postulated that much of the lipid in giardial cells was taken up from the culture media. I did not identify any phosphorylated Cer, nor did I identify inositol containing ceramides. Furthermore, I was unable to confirm the presence of the sphingoid bases, sphingosine or sphinganine. This was primarily due to the lack of a distinct fragmentation profile (both lose H_2O, followed by CH_2O, fragments that are commonly lost by interfering compounds) that could be used to isolate these species from the high noise in the low molecular weight range of the mass spectrometer (m/z 50-350).

This method proved to be quantitative over a narrow linear range and was therefore inappropriate for the quantitation of *Giardia* SLs. To overcome this I standardized an additional

method employing nano-capillary ultra-high pressure liquid chromatography (nano-uHPLC) separation coupled to high resolution mass spectrometry on a bench top orbitrap mass spectrometer (QExactive, Thermo). The LC separation resolved SM, Cer, mono-, di- and tri-hexosylceramides by their fatty acid chains. However once again sphingoid bases did not resolve with this column and therefore they were excluded from the study. Further I was unable to identify the hexosamine containing species using this instrument I believe this is due to a reduction in the extraction of SLs due to a more direct extraction method motivated by the need for quantitation that was not confounded by loss of sample due to processing.

I found that the abundance of Cer and neutral glycosphingolipids increase ~10 fold during encystation, then decrease again in cysts. I also found that SM increases during encystation and remains elevated in cysts with 3 fold increase over trophozoites. Analyses of the species percent composition of culture media and encystation media showed similar profiles to one another, yet both differed from *Giardia* in all life cycle stages, indicating either preferential uptake or the modulation of fatty acid/headgroup by the cell. Interestingly the trend appears to be toward an increase in chain length in the cells as compared with media.

The increase in SM in cysts could potentially indicate a requirement for maintaining cell viability. To assess this, I first separated cysts by density centrifugation, followed by mass spectrometry to identify high SM containing populations and then viability assay using both vital dye incorporation and excystation *in vitro*. I found that there is a correlation between SM concentration and cyst viability using both viability measurement methods. I speculate that high SM allows for modulation of the plasma membrane required for survival outside of the host. Further studies isolating cyst wall and membrane could answer this question and potentially open a wide range of possible targets for the prevention of excystation.

In my dissertation I sought to investigate the SL metabolic enzyme responsible for the regulation of SM. As mentioned above the *Giardia* genome encodes for two acid SMase phosphodiesterase-like 3b precursor enzymes (gASMLPD3b1 and gASMLPD3b2). However given the sequence divergence from characteristic acid and neutral SMase enzymes, including

the lack of SL-binding domain, it was unclear if these enzymes would hydrolyze SM. SL metabolic enzymes are often hydrophobic proteins with extensive post translational modifications, making bacterial recombinant production inappropriate for the synthesis of these enzymes. To circumvent this I used a human coupled *in vitro* translation kit (1 step Human Coupled IVT, Thermo) to synthesize gASMLPD3b1 and gASMLPD3b2. I found that both of these enzymes are functional. gASMLPD3b1 has an acid pH optimum and is inhibited by Zn and possibly Mg. gASMLPD3b2 is active at both acid and neutral pH, with slightly higher activity at acid pH, gASMLPD3b2 is also inhibited by Zn.

Within the cell, SM is likely hydrolyzed to Cer, which is then used as a substrate for the formation of glycosphingolipids beginning with glucosylceramide. Previous reports employing mass spectrometry of proteins have shown that of the two enzymes, gASMLPD3b1 is translated in the cell (Jedelsky *et al.* 2011). Additionally, gASMLPD3b1 was identified as an *N*-glycosylated protein potentially lysosomal or secreted from the cell (Ratner *et al.* 2008). To investigate the enzyme more thoroughly I overexpressed an epitope tagged recombinant under the control of the constitutive alpha-2 tubulin promoter gASMLPD3b1-AU1 in *Giardia* cells. I found that the enzyme inhabits the TVN which has been reported to function as both ER and endosome/lysosome. Given that GlcT1 is likely also an ER resident protein, this fits with the hypothesis that SM is hydrolyzed to Cer which is subsequently glycosylated, all within the ER. In mammalian systems, Cer is trafficked by the Cer Transfer protein (CERT) from the Golgi to the ER, however *Giardia* lacks both Golgi and CERT, therefore it is parsimonious that Cer generation would take place at the site of glucosylceramide generation.

Surprisingly I found gASMLPD3b1 in spent media indicating that this enzyme could be secreted to the environment. Once validated, this could change the paradigm for the causes of membrane dysfunction in epithelial cells co-cultured with G*iardia* trophozoites. Secreted gASMLPD3b1 could potentially decrease membrane barrier function as has been shown with exogenous SMase addition to cultured epithelial cells (Bock *et al.* 2007). However it remains to be seen if gASMLPD3b1 is active within the pH range found in the intestine.

Overexpression of gASMLPD3b1 also lead to decreased excystation efficiency, however excystation was not blocked altogether. Taken together these results suggest that gASMLPD3b1 resides in the TVN where it hydrolyzes SM to Cer for the generation of glucosylceramide. Regulation of this is potentially mediated by the pH of the environment as high pH reduces the activity of this enzyme. Additionally, gASMLPD3b1 is likely processed by cleavage of the transmembrane domain and may be secreted from the cell. Overexpression of this enzyme leads to a reduction in excystation efficiency; however this excess activity is attenuated due to pH requirements of the enzyme. I hypothesize that maintenance of SM at the plasma membrane is carried out by gASMLPD3b2, which has a broader range of activity. Future studies will confirm this by identifying the cellular localization of this enzyme as well as the effect of overexpression on excystation efficiency.

4.1 PROPOSED MODEL

Based on the current results as well as previous reports (Hernandez *et al.* 2007; Abodeely *et al.* 2009; Castillo-Romero *et al.* 2010) a comprehensive model for SL metabolism during encystation has been proposed (Fig 4.1). The model reveals that SLs are taken up from the environment by both clathrin-dependent and -independent endocytic pathways. Cer, either in the extracellular space or produced by activity of gASMLPD3b2, is trafficked to the TVN where it is the substrate for formation of glucosylceramide mediated by gGlcT1. SM is also transported to the TVN where it is hydrolyzed by gASMLPD3b1 to Cer which can then be converted to glucosylceramide. During encystation increased expression of gASMLPD3b1, gASMLPD3b2 and gGlcT1 lead to an increase in the formation of glucosylceramide and this well regulated increase is required for proper formation of ESVs which carry cyst wall material to be deposited on the exterior of the plasma membrane (Mendez, 2013). Di and trihexosylceramide levels also increase and are likely located at the plasma membrane but may potentially aid in the formation of ESVs similar to glucosylceramide. A simultaneous rise in the level of SM and Cer within the cell is likely due to increased uptake and also a result of SM hydrolysis mediated by

gASMLPD3b2 at the plasma membrane stimulating the cytoskeleton-dependent endocytosis. As more SM is brought in, membrane integrity is restored and SM-rich membrane is abundant with detergent resistant domains to support survival of cysts at lower temperature.

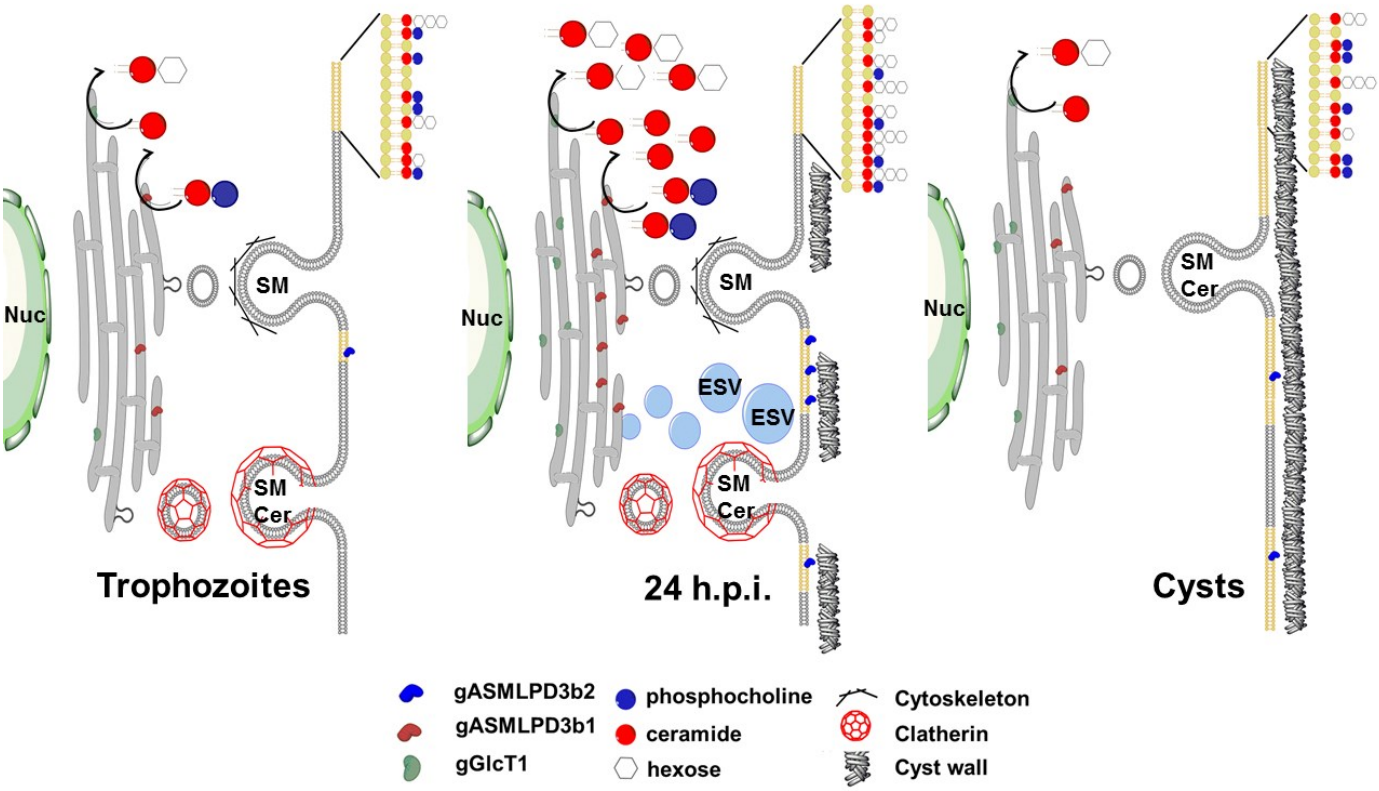

Figure 4.1: Proposed model of Giardia SL metabolism during encystation

Proposed model which shows sphingolipid uptake and metabolism in trophozoites, encysting cells and cysts.

4.2 CONCLUSION AND FUTURE DIRECTION

The sphingolipidome of *G. lamblia* is minimal and composed primarily of lipids which have been scavenged from the environment. Regulation of the incorporation of these lipids

coupled with modulation of their fatty acid and polar head group, allow *Giardia* to fulfill its requirements for these bioactive molecules. I have shown a clear link between the increase in SLs and cyst formation as well as a correlation between SM content and excystation. This is the first time that excystation has been linked with SL and indicates that SLs are critical for all stages of the parasites life cycle. Furthermore I have shown that *Giardia* actively modulate SM levels with both increased uptake and enzymatic hydrolysis. These data suggest that *Giardia* is strongly dependent upon the diet of the host and this could potentially serve as an avenue of investigation for treating the disease. Although it is unlikely that SM could be removed from all diets, especially in infants as it is a major component of human breast milk, the enzymes involved in this pathway are ideal candidates for chemical inhibition. The methods developed in my dissertation open the door for future studies of the lipidome as well as excystation efficiency of *Giardia* which, when coupled with genetic modification of SL genes, will provide valuable insight into potential treatments of this neglected parasite.

References

Abodeely, M., K. N. DuBois, et al. (2009). "A contiguous compartment functions as endoplasmic reticulum and endosome/lysosome in Giardia lamblia." Eukaryot Cell **8**(11): 1665-1676.

Adam, R. D. (2001). "Biology of Giardia lamblia." Clin Microbiol Rev **14**(3): 447-475.

Ankarklev, J., J. Jerlstrom-Hultqvist, et al. (2010). "Behind the smile: cell biology and disease mechanisms of Giardia species." Nat Rev Microbiol **8**(6): 413-422.

Bansal, D., H. S. Bhatti, et al. (2005). "Role of cholesterol in parasitic infections." Lipids Health Dis **4**: 10.

Bartels, T., R. S. Lankalapalli, et al. (2008). "Raftlike mixtures of sphingomyelin and cholesterol investigated by solid-state 2H NMR spectroscopy." J Am Chem Soc **130**(44): 14521-14532.

Ben-David, O. and A. H. Futerman (2010). "The role of the ceramide acyl chain length in neurodegeneration: involvement of ceramide synthases." Neuromolecular Med **12**(4): 341-350.

Bezombes, C., S. Grazide, et al. (2004). "Rituximab antiproliferative effect in B-lymphoma cells is associated with acid-sphingomyelinase activation in raft microdomains." Blood **104**(4): 1166-1173.

Birkeland, S. R., S. P. Preheim, et al. (2010). "Transcriptome analyses of the Giardia lamblia life cycle." Mol Biochem Parasitol **174**(1): 62-65.

Blackwell, A. D., M. Martin, et al. (2013). "Antagonism between two intestinal parasites in humans: the importance of co-infection for infection risk and recovery dynamics." Proc Biol Sci **280**(1769): 20131671.

Blair, R. J. and P. F. Weller (1987). "Uptake and esterification of arachidonic acid by trophozoites of Giardia lamblia." Mol Biochem Parasitol **25**(1): 11-18.

Bock, J., G. Liebisch, et al. (2007). "Exogenous sphingomyelinase causes impaired intestinal epithelial barrier function." World J Gastroenterol **13**(39): 5217-5225.

Boucher, S. E. and F. D. Gillin (1990). "Excystation of in vitro-derived Giardia lamblia cysts." Infect Immun **58**(11): 3516-3522.

Brown, D. M., J. A. Upcroft, et al. (1995). "Free radical detoxification in Giardia duodenalis." Mol Biochem Parasitol **72**(1-2): 47-56.

Castillo-Romero, A., G. Leon-Avila, et al. (2010). "Rab11 and actin cytoskeleton participate in Giardia lamblia encystation, guiding the specific vesicles to the cyst wall." PLoS Negl Trop Dis **4**(6): e697.

Chatterjee, A., A. Carpentieri, et al. (2010). "Giardia cyst wall protein 1 is a lectin that binds to curled fibrils of the GalNAc homopolymer." PLoS Pathog **6**(8).

Ciucanu, I. a. F. K. (1984). "Simple and rapid method for the permethylation of carbohydrates." Carbohydrate Research **131**: 209–217.

Das, S., C. Castillo, et al. (2001). "Phospholipid remodeling/generation in Giardia: the role of the Lands cycle." Trends Parasitol **17**(7): 316-319.

Das, S., D. S. Reiner, et al. (1988). "Killing of Giardia lamblia trophozoites by human intestinal fluid in vitro." J Infect Dis **157**(6): 1257-1260.

Diamond, L. S., D. R. Harlow, et al. (1978). "A new medium for the axenic cultivation of Entamoeba histolytica and other Entamoeba." Trans R Soc Trop Med Hyg **72**(4): 431-432.

DuBois, K. N., M. Abodeely, et al. (2008). "Identification of the major cysteine protease of Giardia and its role in encystation." J Biol Chem **283**(26): 18024-18031.
Eckmann, L., F. Laurent, et al. (2000). "Nitric oxide production by human intestinal epithelial cells and competition for arginine as potential determinants of host defense against the lumen-dwelling pathogen Giardia lamblia." J Immunol **164**(3): 1478-1487.
Faso, C. and A. B. Hehl (2011). "Membrane trafficking and organelle biogenesis in Giardia lamblia: use it or lose it." Int J Parasitol **41**(5): 471-480.
Fornoni, A., J. Sageshima, et al. (2011). "Rituximab targets podocytes in recurrent focal segmental glomerulosclerosis." Sci Transl Med **3**(85): 85ra46.
Futerman, A. H. and H. Riezman (2005). "The ins and outs of sphingolipid synthesis." Trends Cell Biol **15**(6): 312-318.
Gerwig, G. J., J. A. van Kuik, et al. (2002). "The Giardia intestinalis filamentous cyst wall contains a novel beta(1-3)-N-acetyl-D-galactosamine polymer: a structural and conformational study." Glycobiology **12**(8): 499-505.
Gibson, G. R., D. Ramirez, et al. (1999). "Giardia lamblia: incorporation of free and conjugated fatty acids into glycerol-based phospholipids." Exp Parasitol **92**(1): 1-11.
Gillin, F. D. (1987). "Giardia lamblia: the role of conjugated and unconjugated bile salts in killing by human milk." Exp Parasitol **63**(1): 74-83.
Gillin, F. D., S. E. Boucher, et al. (1989). "Giardia lamblia: the roles of bile, lactic acid, and pH in the completion of the life cycle in vitro." Exp Parasitol **69**(2): 164-174.
Gillin, F. D., M. J. Gault, et al. (1986). "Biliary lipids support serum-free growth of Giardia lamblia." Infect Immun **53**(3): 641-645.
Goni, F. M. and A. Alonso (2002). "Sphingomyelinases: enzymology and membrane activity." FEBS Lett **531**(1): 38-46.
Gottig, N., E. V. Elias, et al. (2006). "Active and passive mechanisms drive secretory granule biogenesis during differentiation of the intestinal parasite Giardia lamblia." J Biol Chem **281**(26): 18156-18166.
Grosch, S., S. Schiffmann, et al. (2012). "Chain length-specific properties of ceramides." Prog Lipid Res **51**(1): 50-62.
Halliez, M. C. and A. G. Buret (2013). "Extra-intestinal and long term consequences of Giardia duodenalis infections." World J Gastroenterol **19**(47): 8974-8985.
Hannun, Y. A. and L. M. Obeid (2008). "Principles of bioactive lipid signalling: lessons from sphingolipids." Nat Rev Mol Cell Biol **9**(2): 139-150.
Hernandez, Y., C. Castillo, et al. (2007). "Clathrin-dependent pathways and the cytoskeleton network are involved in ceramide endocytosis by a parasitic protozoan, Giardia lamblia." Int J Parasitol **37**(1): 21-32.
Hernandez, Y., M. Shpak, et al. (2008). "Novel role of sphingolipid synthesis genes in regulating giardial encystation." Infect Immun **76**(7): 2939-2949.
Hilario, E. and J. P. Gogarten (1998). "The prokaryote-to-eukaryote transition reflected in the evolution of the V/F/A-ATPase catalytic and proteolipid subunits." J Mol Evol **46**(6): 703-715.
House, S. A., D. J. Richter, et al. (2011). "Giardia flagellar motility is not directly required to maintain attachment to surfaces." PLoS Pathog **7**(8): e1002167.
Hsu, F. F. and J. Turk (2000). "Structural determination of sphingomyelin by tandem mass spectrometry with electrospray ionization." J Am Soc Mass Spectrom **11**(5): 437-449.

Huang, Y. C., L. H. Su, et al. (2008). "Regulation of cyst wall protein promoters by Myb2 in Giardia lamblia." J Biol Chem **283**(45): 31021-31029.
Jarroll, E. L., P. J. Muller, et al. (1981). "Lipid and carbohydrate metabolism of Giardia lamblia." Mol Biochem Parasitol **2**(3-4): 187-196.
Jedelsky, P. L., P. Dolezal, et al. (2011). "The minimal proteome in the reduced mitochondrion of the parasitic protist Giardia intestinalis." PLoS One **6**(2): e17285.
Jiang, X., H. Cheng, et al. (2007). "Alkaline methanolysis of lipid extracts extends shotgun lipidomics analyses to the low-abundance regime of cellular sphingolipids." Anal Biochem **371**(2): 135-145.
Kaneda, Y. and T. Goutsu (1988). "Lipid analysis of Giardia lamblia and its culture medium." Ann Trop Med Parasitol **82**(1): 83-90.
Karanis, P., C. Kourenti, et al. (2007). "Waterborne transmission of protozoan parasites: a worldwide review of outbreaks and lessons learnt." J Water Health **5**(1): 1-38.
Keister, D. B. (1983). "Axenic culture of Giardia lamblia in TYI-S-33 medium supplemented with bile." Trans R Soc Trop Med Hyg **77**(4): 487-488.
Kramer, M. H., B. L. Herwaldt, et al. (1996). "Surveillance for waterborne-disease outbreaks--United States, 1993-1994." MMWR CDC Surveill Summ **45**(1): 1-33.
Lauwaet, T., B. J. Davids, et al. (2007). "Encystation of Giardia lamblia: a model for other parasites." Curr Opin Microbiol **10**(6): 554-559.
Levery, S. B. (2005). "Glycosphingolipid structural analysis and glycosphingolipidomics." Methods Enzymol **405**: 300-369.
Li, Y., S. Teneberg, et al. (2008). "Sensitive detection of isoglobo and globo series tetraglycosylceramides in human thymus by ion trap mass spectrometry." Glycobiology **18**(2): 158-165.
Lindmark, D. G. (1980). "Energy metabolism of the anaerobic protozoon Giardia lamblia." Mol Biochem Parasitol **1**(1): 1-12.
Lingwood, D. and K. Simons (2010). "Lipid rafts as a membrane-organizing principle." Science **327**(5961): 46-50.
Liu, B., L. M. Obeid, et al. (1997). "Sphingomyelinases in cell regulation." Semin Cell Dev Biol **8**(3): 311-322.
Loidl, A., R. Claus, et al. (2002). "High-precision fluorescence assay for sphingomyelinase activity of isolated enzymes and cell lysates." J Lipid Res **43**(5): 815-823.
Lopez, A. B., K. Sener, et al. (2007). "UDP-N-acetylglucosamine 4'-epimerase from the intestinal protozoan Giardia intestinalis lacks UDP-glucose 4'-epimerase activity." J Eukaryot Microbiol **54**(2): 154-160.
Maia-Brigagao, C., J. A. Morgado-Diaz, et al. (2012). "Giardia disrupts the arrangement of tight, adherens and desmosomal junction proteins of intestinal cells." Parasitol Int **61**(2): 280-287.
Mendez, T. L., A. De Chatterjee, et al. (2013). "Glucosylceramide transferase activity is critical for encystation and viable cyst production by an intestinal protozoan, Giardia lamblia." J Biol Chem **288**(23): 16747-16760.
Mohareb, E. W., E. J. Rogers, et al. (1991). "Giardia lamblia: phospholipid analysis of human isolates." Ann Trop Med Parasitol **85**(6): 591-597.
Morf, L., C. Spycher, et al. (2010). "The transcriptional response to encystation stimuli in Giardia lamblia is restricted to a small set of genes." Eukaryot Cell **9**(10): 1566-1576.

Morrison, H. G., A. G. McArthur, et al. (2007). "Genomic minimalism in the early diverging intestinal parasite Giardia lamblia." Science **317**(5846): 1921-1926.
Obeid, L. M. and Y. A. Hannun (1995). "Ceramide: a stress signal and mediator of growth suppression and apoptosis." J Cell Biochem **58**(2): 191-198.
Ogretmen, B. and Y. A. Hannun (2004). "Biologically active sphingolipids in cancer pathogenesis and treatment." Nat Rev Cancer **4**(8): 604-616.
Pan, Y. J., C. C. Cho, et al. (2009). "A novel WRKY-like protein involved in transcriptional activation of cyst wall protein genes in Giardia lamblia." J Biol Chem **284**(27): 17975-17988.
Perez, P. F., J. Minnaard, et al. (2001). "Inhibition of Giardia intestinalis by extracellular factors from Lactobacilli: an in vitro study." Appl Environ Microbiol **67**(11): 5037-5042.
Pernet, F., C. J. Pelletier, et al. (2006). "Comparison of three solid-phase extraction methods for fatty acid analysis of lipid fractions in tissues of marine bivalves." J Chromatogr A **1137**(2): 127-137.
Prucca, C. G. and H. D. Lujan (2009). "Antigenic variation in Giardia lamblia." Cell Microbiol **11**(12): 1706-1715.
Punta, M., P. C. Coggill, et al. (2012). "The Pfam protein families database." Nucleic Acids Res **40**(Database issue): D290-301.
Ratner, D. M., J. Cui, et al. (2008). "Changes in the N-glycome, glycoproteins with Asn-linked glycans, of Giardia lamblia with differentiation from trophozoites to cysts." Eukaryot Cell **7**(11): 1930-1940.
Rayan, P., D. Stenzel, et al. (2005). "The effects of saturated fatty acids on Giardia duodenalis trophozoites in vitro." Parasitol Res **97**(3): 191-200.
Regoes, A., D. Zourmpanou, et al. (2005). "Protein import, replication, and inheritance of a vestigial mitochondrion." J Biol Chem **280**(34): 30557-30563.
Reiner, D. S., M. McCaffery, et al. (1990). "Sorting of cyst wall proteins to a regulated secretory pathway during differentiation of the primitive eukaryote, Giardia lamblia." Eur J Cell Biol **53**(1): 142-153.
Reiner, D. S., C. S. Wang, et al. (1986). "Human milk kills Giardia lamblia by generating toxic lipolytic products." J Infect Dis **154**(5): 825-832.
Ringqvist, E., J. E. Palm, et al. (2008). "Release of metabolic enzymes by Giardia in response to interaction with intestinal epithelial cells." Mol Biochem Parasitol **159**(2): 85-91.
Scarlatti, F., C. Bauvy, et al. (2004). "Ceramide-mediated macroautophagy involves inhibition of protein kinase B and up-regulation of beclin 1." J Biol Chem **279**(18): 18384-18391.
Schofield, P. J., M. R. Edwards, et al. (1992). "The pathway of arginine catabolism in Giardia intestinalis." Mol Biochem Parasitol **51**(1): 29-36.
Simons, K. and M. J. Gerl (2010). "Revitalizing membrane rafts: new tools and insights." Nat Rev Mol Cell Biol **11**(10): 688-699.
Simons, K. and J. L. Sampaio (2011). "Membrane organization and lipid rafts." Cold Spring Harb Perspect Biol **3**(10): a004697.
Singer, S. M. and T. E. Nash (2000). "The role of normal flora in Giardia lamblia infections in mice." J Infect Dis **181**(4): 1510-1512.
Slavin, I., A. Saura, et al. (2002). "Dephosphorylation of cyst wall proteins by a secreted lysosomal acid phosphatase is essential for excystation of Giardia lamblia." Mol Biochem Parasitol **122**(1): 95-98.
Slotte, J. P. (2013). "Biological functions of sphingomyelins." Prog Lipid Res **52**(4): 424-437.

Smith, A. L. and H. V. Smith (1989). "A comparison of fluorescein diacetate and propidium iodide staining and in vitro excystation for determining Giardia intestinalis cyst viability." Parasitology **99 Pt 3**: 329-331.

Sonda, S., S. Stefanic, et al. (2008). "A sphingolipid inhibitor induces a cytokinesis arrest and blocks stage differentiation in Giardia lamblia." Antimicrob Agents Chemother **52**(2): 563-569.

Stechmann, A. and T. Cavalier-Smith (2002). "Rooting the eukaryote tree by using a derived gene fusion." Science **297**(5578): 89-91.

Stefanic, S., D. Palm, et al. (2006). "Organelle proteomics reveals cargo maturation mechanisms associated with Golgi-like encystation vesicles in the early-diverged protozoan Giardia lamblia." J Biol Chem **281**(11): 7595-7604.

Stefanic, S., C. Spycher, et al. (2010). "Glucosylceramide synthesis inhibition affects cell cycle progression, membrane trafficking, and stage differentiation in Giardia lamblia." J Lipid Res **51**(9): 2527-2545.

Stevens, T. L., G. R. Gibson, et al. (1997). "Uptake and cellular localization of exogenous lipids by Giardia lamblia, a primitive eukaryote." Exp Parasitol **86**(2): 133-143.

Subramanian, A. B., S. Navarro, et al. (2000). "Role of exogenous inositol and phosphatidylinositol in glycosylphosphatidylinositol anchor synthesis of GP49 by Giardia lamblia." Biochim Biophys Acta **1483**(1): 69-80.

Sullards, M. C., J. C. Allegood, et al. (2007). "Structure-specific, quantitative methods for analysis of sphingolipids by liquid chromatography-tandem mass spectrometry: "inside-out" sphingolipidomics." Methods Enzymol **432**: 83-115.

Talal, A. H. and J. A. Murray (1994). "Acute and chronic diarrhea. How to keep laboratory testing to a minimum." Postgrad Med **96**(3): 30-32, 35-38, 43 passim.

Vanier, M. T. (2013). "Niemann-Pick diseases." Handb Clin Neurol **113**: 1717-1721.

Vargas-Villarreal, J., B. L. Escobedo-Guajardo, et al. (2007). "Activity of intracellular phospholipase A1 and A2 in Giardia lamblia." J Parasitol **93**(5): 979-984.

Venable, M. E., J. Y. Lee, et al. (1995). "Role of ceramide in cellular senescence." J Biol Chem **270**(51): 30701-30708.

Ward, W., L. Alvarado, et al. (1997). "A primitive enzyme for a primitive cell: the protease required for excystation of Giardia." Cell **89**(3): 437-444.

Watkins, R. R. and L. Eckmann (2014). "Treatment of giardiasis: current status and future directions." Curr Infect Dis Rep **16**(2): 396.

WHO (2013). Diarrhoeal disease, World Health Organization.

Yichoy, M., T. T. Duarte, et al. (2010). "Lipid metabolism in Giardia: a post-genomic perspective." Parasitology: 1-12.

Yichoy, M., E. S. Nakayasu, et al. (2009). "Lipidomic analysis reveals that phosphatidylglycerol and phosphatidylethanolamine are newly generated phospholipids in an early-divergent protozoan, Giardia lamblia." Mol Biochem Parasitol **165**(1): 67-78.

Zeidan, Y. H. and Y. A. Hannun (2010). "The acid sphingomyelinase/ceramide pathway: biomedical significance and mechanisms of regulation." Curr Mol Med **10**(5): 454-466.

Vita

Trevor T. Duarte earned his Bachelor of Science Degree in Microbiology from the University of Texas at El Paso in 2007. The following year he joined the Pathobiology doctoral program in Biological Science at the University of Texas at El Paso. Trevor has received an NIH research fellowship from the RISE program as well as honorable mention from the NSF pre-doctoral fellowship. While pursuing his degree he worked as an NIH grant supported research assistant for Dr. Siddhartha Das in the Biological Science department. To that end he mentored numerous undergraduate students and was one of a handful of students qualified to operate the Biomolecule Analysis Core Facilities' mass spectrometers.

Trevor has presented his research at numerous international conferences including the International Conference of Anaerobic Parasites, the 22nd and 24th annual Molecular Parasitology Meeting and the LipidMaps Meeting for Lipidomics Impact on Cell Biology, Inflammation and Metabolic Diseases. Additionally his research has been published in *Infection and Immunity* as well as *The Journal of Biological Chemistry* His dissertation, *Global Sphingolipid Profile of Giardia lamblia During Stage Differentiation: The influence of Sphingomyelin Abundance on Viable Cyst Production,* was supervised by Dr. Siddhartha Das.

Permanent address: 6537 Fiesta Dr.
El Paso, TX, 79912

This dissertation was typed by Trevor T. Duarte